Investigation of 1,900 Individual Field Aged Photovoltaic Modules for Potential Induced Degradation (PID) in a Positive Biased Power Plant

by

Jaspreet Singh

A Thesis Presented in Partial Fulfillment
of the Requirements for the Degree of
Master of Science in Technology

Approved November 2011 by the
Graduate Supervisory Committee:

Govindasamy Tamizhmani, Chair
Devarajan Srinivasan
Bradley Rogers

ARIZONA STATE UNIVERSITY

December 2011

ABSTRACT

Photovoltaic (PV) modules undergo performance degradation depending on climatic conditions, applications, and system configurations. The performance degradation prediction of PV modules is primarily based on Accelerated Life Testing (ALT) procedures. In order to further strengthen the ALT process, additional investigation of the power degradation of field aged PV modules in various configurations is required. A detailed investigation of 1,900 field aged (12-18 years) PV modules deployed in a power plant application was conducted for this study. Analysis was based on the current-voltage (I-V) measurement of all the 1,900 modules individually. I-V curve data of individual modules formed the basis for calculating the performance degradation of the modules. The percentage performance degradation and rates of degradation were compared to an earlier study done at the same plant. The current research was primarily focused on identifying the extent of potential induced degradation (PID) of individual modules with reference to the negative ground potential. To investigate this, the arrangement and connection of the individual modules/strings was examined in detail. The study also examined the extent of underperformance of every series string due to performance mismatch of individual modules in that string. The power loss due to individual module degradation and module mismatch at string level was then compared to the rated value.

DEDICATION

I would like to dedicate this thesis to my beloved grandmothers, late Baljit Kaur Kang and late Harbans Kaur. It is only because of their blessings and love that I have reached where I am today.

ACKNOWLEDGMENTS

A formal statement of acknowledgement is hardly sufficient to express my gratitude towards the personalities who have helped me in undertaking and completing this work.

First, I would thank Dr. GovindaSamy TamizhMani for granting me permission to work as a research assistant on this prestigious project and for providing guidance and support throughout the project. I would also like to thank Dr. Devarajan Srinivasan and Dr. Bradley B. Rogers for reviewing the project and showing interest in my work.

I owe equal thanks to Jim Piotrowski and Cassius Mcchesney for their support at the APS Solar Test and Research Center. Their cooperation was vital for the completion of this project.

I am forever indebted to my colleague Jonathan Belmont for helping me with data collection during the harsh summer months. He supported me on a professional and a personal level during the course of this project. I am also extremely thankful to my friends Manishkumar Jha and Hitendra Pratap Singh for helping me with the data extraction process and for IT support.

Lastly, I would like to thank my friend Hardeep Singh and my roommate Ramandeep Singh for standing beside me and supporting me through the hard times.

TABLE OF CONTENTS

CHAPTER Page

LIST OF TABLES

LIST OF FIGURES

Figure Page

Figure Page

Figure Page

CHAPTER 1

INTRODUCTION

1. 1 Background

Crystalline silicon photovoltaic (PV) modules typically degrade at an average rate of 0.5-0.7% per year [1]. Thus, the degradation rate of a PV module impacts the total energy generation potential of the system. Several factors have an impact on the performance degradation of a PV module when exposed to real life conditions. These factors can be broadly classified in two categories: intrinsic and extrinsic. The intrinsic factors for degradation of a typical PV module are its material, construction, and design. Extrinsic elements, such as temperature and moisture, also significantly impact the performance degradation of a PV module. Recent studies suggest that the system design in which a PV module is installed also needs to be studied to better understand the performance degradation of field-aged modules [2].

Reliability assessment of a PV module relies heavily on Accelerated Life Testing (ALT) procedures. In order to make these procedures more productive and accurate, further research needs to be conducted on the factors affecting the fielded PV modules at the module, string, and system levels.

The hot and dry climate of Tempe, Arizona, and the availability of 12-18-year-old field aged PV modules in an operating power plant were the key ingredients for this research.

1.2 Objective

The specific objective of this study was to investigate approximately 1,900 field aged PV modules, at both individual and string levels. The main focus was to substantiate three primary results:

1. Potential Induced Degradation (PID) in a positive biased and negative grounded power plant;
2. Power drop at system and string level due to module mismatch in series connected modules; and
3. Performance degradation of 1,900 modules in a grid-tied operation in the hot and dry climate of Arizona.

The results and findings of this study will be highly beneficial to the PV industry and this study will allow:

- the industry to understand if there is any real influence of system voltage and ground potential on the durability and reliability of PV modules;
- the industry to understand how the string power is affected by the power output of field aged/mismatched individual modules;
- the industry to better predict the lifetime of the PV modules and develop superior products;
- the customers to have confidence in the reliability and performance of the modules over the period of time guaranteed to them; and
- the researchers to look for new avenues and subjects in performance degradation studies.

1.3 Scope of the Project

The scope of this project is depicted below in Figure 1. The two perspectives of this study were reliability and electrical performance. Current- voltage (I-V) curves were taken over a period of six months on all the 1,900 modules. This included the I-V measurements at string levels as well. Baseline performance curves were also taken to obtain the temperature coefficients of each model/type. Detailed drawings and circuit diagrams were prepared as a part of analysis work as well. All of these processes were interlinked and the results were analyzed.

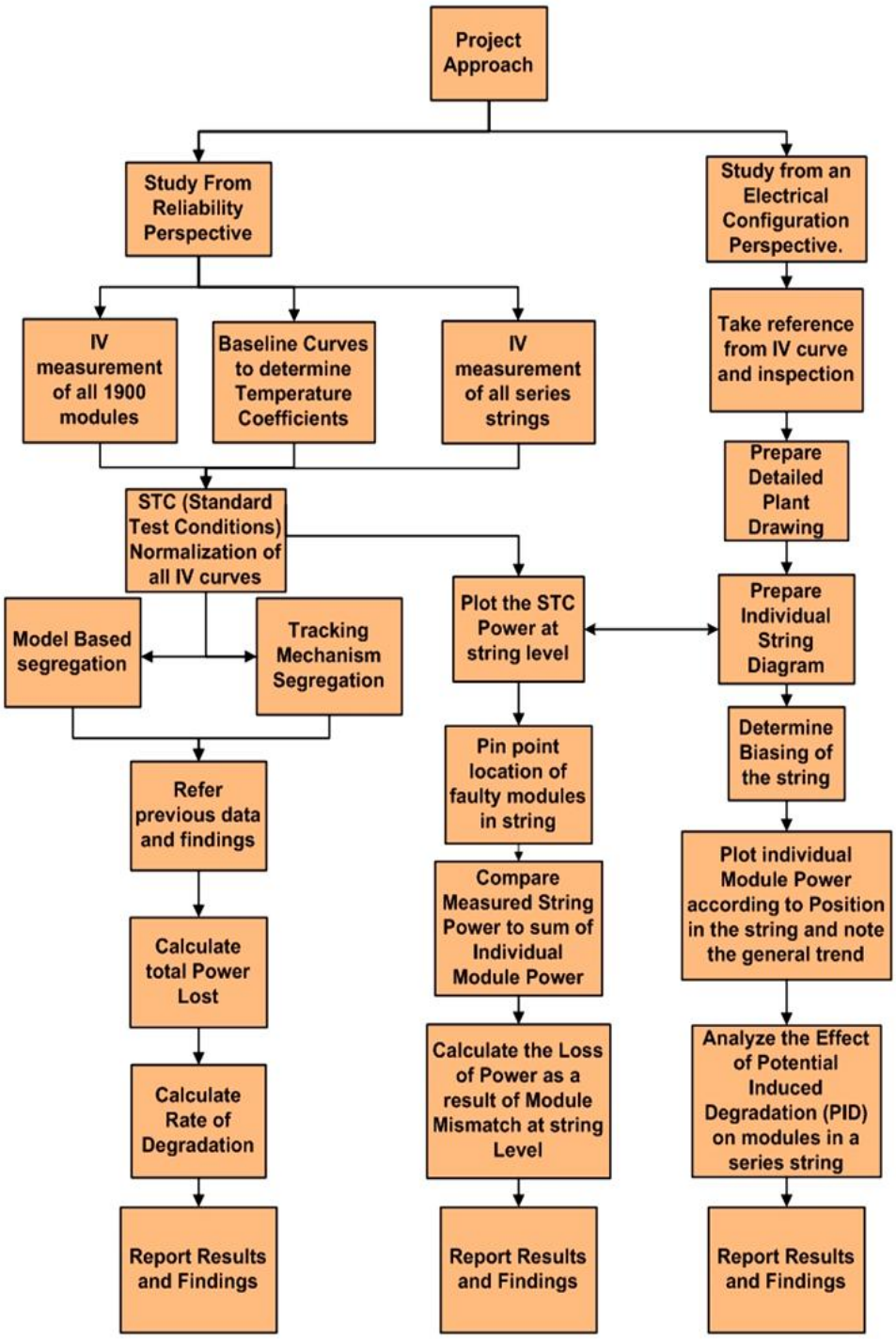

Figure 1.1 Scope of the project

CHAPTER 2

LITERATURE REVIEW

2.1 Performance degradation measurement

Reliability study of a PV module is important from a technical and marketing perspective [3]. Whether or not a module will be able to perform at its rated value for the promised amount of time is the primary concern of any reliability program [3]. Most of the reliability programs existing today are able to minimize the failure rates during the start of the lifetime of a module, as shown in Figure 2 below. The failure rate of a module is known to increase exponentially towards the end of its life. Therefore, an in-depth study in this field is required to predict more accurately the lifetime of a PV module.

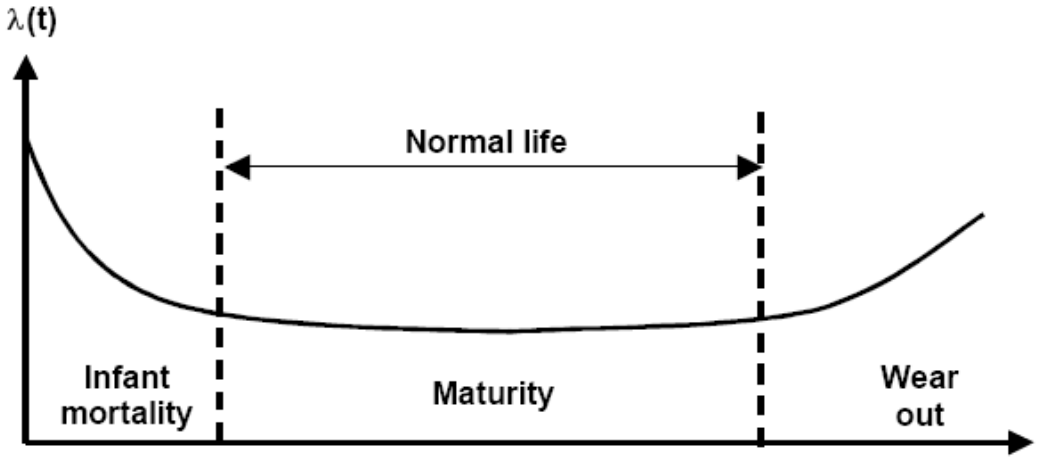

Figure 2.1 Bathtub curve depicting PV failure rates [7]

The basis of most reliability studies is accelerated testing [4]. Accelerated testing is done by manufacturers, testing laboratories and research laboratories to accurately confirm the performance and safety standards of a PV module over a period of time [3, 4, 5]. Accelerated life testing involves testing of modules in a laboratory setting, where harsh outdoor conditions are created in the form of

stresses to replicate the environmental effects. Processes such as thermal cycling, damp heat, humidity freeze, mechanical load (static and dynamic), and hot spot endurance tests are the crux of qualification and reliability testing of PV modules [3, 7].

The qualification test standards IEC 61215 and IEC 61646 [8, 9] have been successful in replicating the initial field failure mechanisms of a PV module [4]. However, due to the increasing need for more accurate lifetime predictions, field aged modules need to be investigated further [3, 4, 5]. The pertinent field data is used to understand the various stress levels experienced by a PV module under certain conditions. These stress levels are then used to design acceleration factors for qualification and reliability testing. These acceleration factors then form the basis for testing new and emerging products [5].

2.2 Module versus String Evaluation

Most reliability studies are conducted from an individual module's perspective. Accelerated tests and other qualification standards define the test methods for individual modules. However, a module may be subjected to varying phenomena when it is part of a string. A string is a combination of a series or parallel modules. Strings are created to combine voltage (series) and current (parallel) for higher power output. Random modules in a string can induce random current/voltage values. Due to the series connection configuration, the total current in that string would be equal to or lower than the lowest current producing module of that particular string [10]. Thus, the whole string is bound to perform at the behest of the weakest module in the respective string. This curtails the power output from a better performing module/modules and drops the power output of the particular string.

Researchers have observed that degradation of modules over time causes reduced power output. This decrease can be up to 12% for field aged modules [11]. This power drop at the string level can be due to environmental factors or performance differences between modules. Overall, the string power would be less than the sum of individual module powers of that string. This is referenced as mismatch loss [11].

The flow of low current in the array can be due to several causes, including shading issue, encapsulant browning, or a damaged cell [12]. The damaged/shaded cell in a module would then act as a load, rather than a generator [12]. The load would then dissipate power in the form of heat, and this localized heating in a cell/module might create hotspots in the module [12]. Depending on the location of a hotspot, degradation can be further invigorated. If created at a critical spot in the module, a hotspot might lead to generation of arcing and, eventually, a fire. This situation can be worse in a power plant setting where a large number of strings are connected to achieve higher power generation.

Understanding the effects of module mismatch—whether existing from the beginning or created over the passage of time—is thus necessary from a reliability and safety perspective. The existence of a 190 kW power plant aged 12-18 years at the APS STAR center provided a good opportunity to study and analyze the extent of mismatch loss.

2.3 Potential Induced Degradation (PID)

As explained in the previous section, modules are connected in series and parallel circuits to create a higher power output at a PV power plant. The series

arrangement exposes the modules at the extreme ends to different voltage levels [13]. This voltage difference can be in the order of several hundred volts [13].

In the case of framed modules in a PV array, equipment grounding is performed as a safety precaution [14]. Figure 2.2 explains the grounding techniques used in PV systems. This again exposes the modules in a series to high voltage biasing [15]. Depending on the grounding methods, a string can be either negative grounded, positive grounded, or floating.

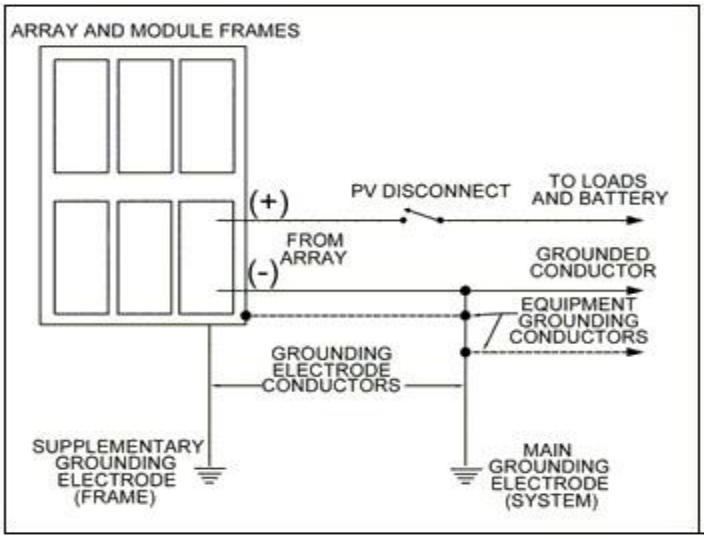

Figure 2.2 Equipment and system grounding [16]

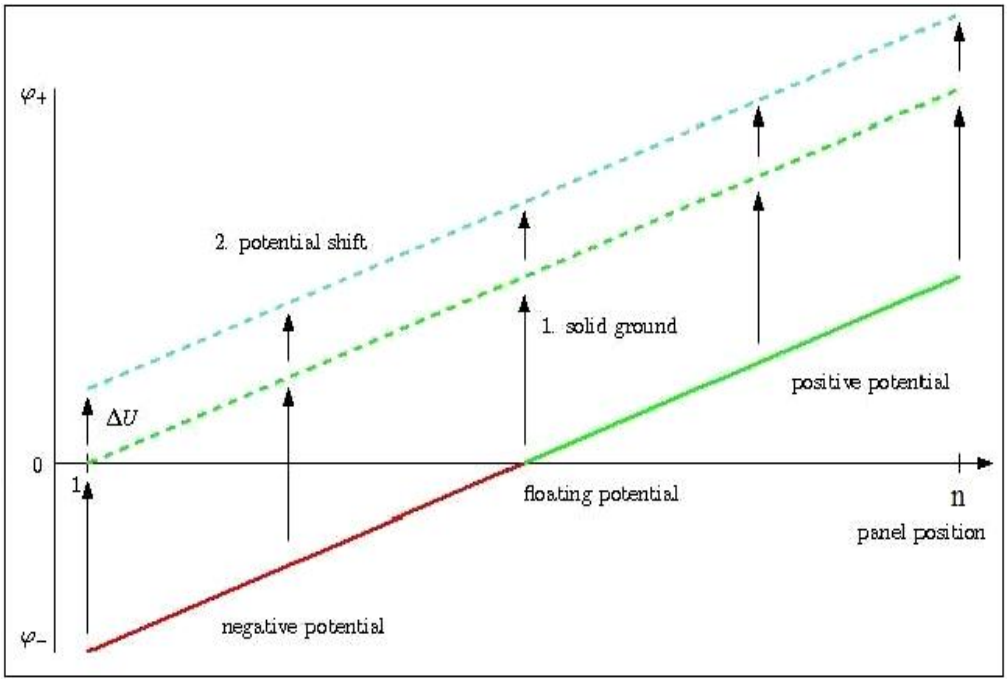

Figure 2.3 Determination of biasing technique in a series string with grounding [17]

Figure 2.3 provides an example for determining the biasing of a string. A system where the negative end of the string is grounded becomes a positive biased string. Similarly, a positive grounded string becomes a negatively biased string. Biasing in a string with high voltages produces a flow of leakage current in the string.

Leakage current can thus flow through the superstrates and/or the encapsulant (insulation) into the ground. This leakage current (less than one mA), can hamper the long-term durability of the PV module [13], a phenomenon called Potential Induced Degradation (PID) [13]. PID is mostly found in power plants where the modules are combined in a series to obtain high voltage levels. This means the effect of system bias voltage increases on the panel, module, and cell [17]. Thus, PID is studied separately for cell level, module level, and system level [17].

The range of potential difference between modules at two extreme ends of string can vary. In the USA, it can be up to ±600 volts with respect to ground, whereas in Europe and other places, it can be up to ±1000 volts with respect to ground [18]. In a recent study at the Florida Solar Energy Center, the power degradation of biased modules installed for 1.5 years ranged from 8% (+1500V) to 25.6% (-1500V). This clearly shows that the degradation of modules is affected by voltage bias. Other factors that strongly influence the PID of fielded modules include, but are not limited to, material, relative humidity/moisture, temperature, grounding (bias), and voltage level [15, 17, 18, 19].

The study of PID effect on modules becomes critical from a safety, durability, and reliability perspective. The flow of leakage current through the insulation of the module can affect its dielectric properties over the long term. Failure of insulation would mean exposure to dc currents and generation of a spark at any weak point in the module. This could develop into a fire hazard and jeopardize the safety of personnel and property [16].

The industry will benefit immensely by the creation of a product with higher isolation capability to counter the effect of PID. This can be a vital selling point and a technical benchmark for the industry. This study would also enable reliability engineers to redesign their accelerated testing and introduce new tests/techniques based on the modified acceleration factors [15]. These techniques and procedures would prove helpful in predicting the lifetime and reliability of a module with higher precision and accuracy, which would then result in better quality and a stronger warranty for the finished product.

The intention of this work is to record the performance degradation and to quantitatively identify the extent of potential induced degradation (PID) of

individual modules of any string with reference to ground potential of a power plant composed of about 1,900 field aged (12-18 years) c-Si modules.

CHAPTER 3

METHODOLOGY

3.1 Data collection

3.1.1 I-V measurements of individual modules

The methodology for the investigation of fielded PV modules in a photovoltaic power plant required the measurement of I-V data for all the modules. The I-V data forms the basis for studying the electrical characteristics of these modules. Each of the 1,855 modules was cleaned, washed, and allowed to dry before each measurement to ensure that the soiling effect of the module did not underrate the measured power. In this study, different monocrystalline silicon (mono-Si) and polycrystalline silicon (poly-Si) were investigated. The modules also had different construction and design (Double Glass/ Glass Polymer). This analysis is thus a mix of different types of examinations on an existing PV power plant.

First, the ac disconnect and dc disconnect switches were turned off and the array was disconnected from the power plant. To measure each individual module, the module was open circuited by disconnecting it from the respective string. Some modules in the power plant, however, could not be measured due to various termination/connection issues.

3.1.2 String I-V measurement

A large number of modules were connected in series to achieve higher voltage levels in the power plant. If the power outputs of the modules differ from each other, the module mismatch effect is introduced. Thus, the I-V curve data for each string was measured. The row containing the string was first disconnected

from the power plant and measurement was taken at the junction box where the strings are combined.

3.1.3 Equipment Used

A Daystar DS 100C I-V curve tracer was used to measure the I-V data for each individual module and individual strings (described in Figure 3.1). The length of connection cables from the tracer to the modules remained constant (one meter) throughout the study to minimize the effect of voltage drop due to cable length.

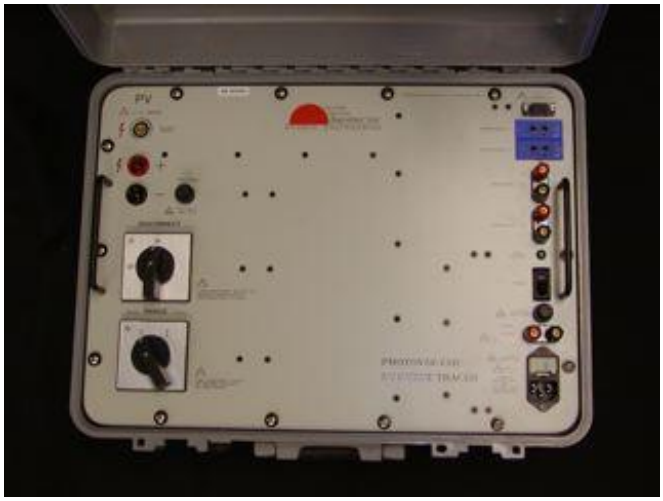

Figure 3.1 Daystar DS-100C curve tracer [20]

A set of reference cells were used to measure the irradiance level at the plant; they comprised the same cell technology (c-Si) as the modules being measured. The reference cells were mounted on the same plane as the module being measured. Thermocouples on the reference cell were used to measure the reference cell temperature. The back sheet of the module was measured using another thermocouple connected directly to the tracer. The ambient temperature was recorded using an additional thermocouple directly mounted on the tracer.

3.2 Data Normalization

3.2.1 Baseline Data Collection

Baseline data is essential for calculating the temperature coefficients for voltage (β), current (α), and power. Ten I-V curves were taken on each module type. As the modules were installed at the power plant, they were cooled onsite using water and icepacks. They were later dried and measured using the Daystar DS-100 C curve tracer. A two-inch thick Styrofoam sheet (Figure 3.2) was used to cover each module before exposing it to the sun. This process ensured that the temperature of the module incremented slowly from about 25°C to 45°C. The irradiance was approximately 1,000 watts/m^2 during the whole process.

Figure 3.2 Baseline testing of one of the modules

3.2.2 Translation procedure

Data was collected in the ambient conditions existing at the power plant over a six-month period. Across such a long period, weather conditions differ significantly. The measured I-V curves were normalized using an automated Microsoft Excel spreadsheet developed at Arizona State University (ASU), shown in Figure 3.3.

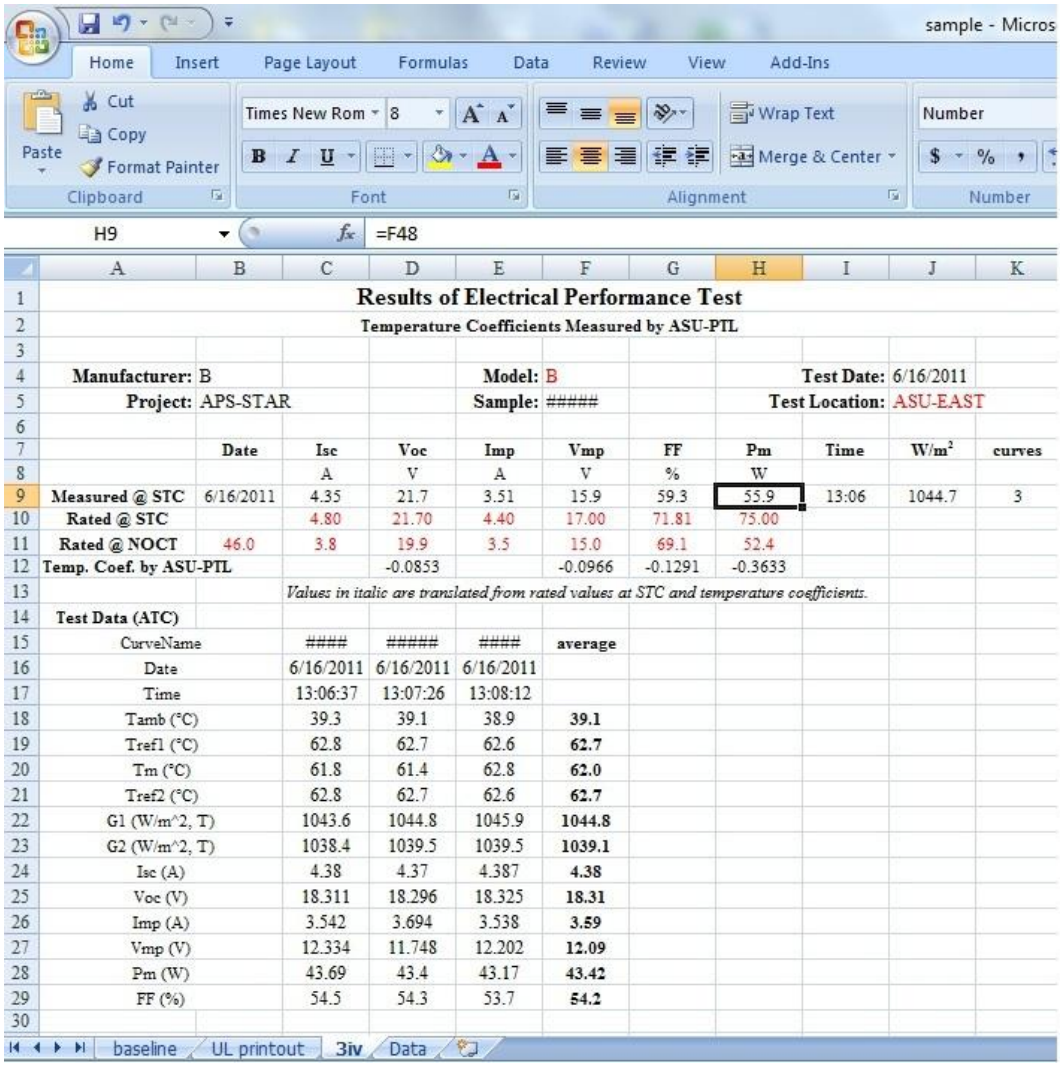

Results of Electrical Performance Test

Temperature Coefficients Measured by ASU-PTL

Manufacturer:	B			**Model:**	B			**Test Date:**	6/16/2011	
Project:	APS-STAR			**Sample:**	#####			**Test Location:**	ASU-EAST	
	Date	**Isc**	**Voc**	**Imp**	**Vmp**	**FF**	**Pm**	**Time**	**W/m²**	**curves**
		A	V	A	V	%	W			
Measured @ STC	6/16/2011	4.35	21.7	3.51	15.9	59.3	55.9	13:06	1044.7	3
Rated @ STC		4.80	21.70	4.40	17.00	71.81	75.00			
Rated @ NOCT	46.0	3.8	19.9	3.5	15.0	69.1	52.4			
Temp. Coef. by ASU-PTL			-0.0853		-0.0966	-0.1291	-0.3633			

Values in italic are translated from rated values at STC and temperature coefficients.

Test Data (ATC)					
CurveName	####	#####	####	**average**	
Date	6/16/2011	6/16/2011	6/16/2011		
Time	13:06:37	13:07:26	13:08:12		
Tamb (°C)	39.3	39.1	38.9	**39.1**	
Tref1 (°C)	62.8	62.7	62.6	**62.7**	
Tm (°C)	61.8	61.4	62.8	**62.0**	
Tref2 (°C)	62.8	62.7	62.6	**62.7**	
G1 (W/m^2, T)	1043.6	1044.8	1045.9	**1044.8**	
G2 (W/m^2, T)	1038.4	1039.5	1039.5	**1039.1**	
Isc (A)	4.38	4.37	4.387	**4.38**	
Voc (V)	18.311	18.296	18.325	**18.31**	
Imp (A)	3.542	3.694	3.538	**3.59**	
Vmp (V)	12.334	11.748	12.202	**12.09**	
Pm (W)	43.69	43.4	43.17	**43.42**	
FF (%)	54.5	54.3	53.7	**54.2**	

Figure 3.3 ASU translation procedure for data normalization

The sheet in Figure 3.4 contains variable and non-variable cells. The measured I-V curves from APS STAR were transferred into the Excel spreadsheet, otherwise known as the three curve translation method. The coefficients used for translations were calculated from the baseline curves of the respective module type.

The Excel spreadsheet thus provided the translated STC data for current, voltage, and power. This translated data was used further in the analysis process

to calculate module degradation, mismatch calculation, and Potential Induced Degradation (PID) studies.

3.3 Plant Layout and String Circuit Diagram

3.3.1 Detailed Plant Layout

To segregate and analyze the modules based on module type and tracking mechanism and to create the string level diagrams, a detailed overview of the plant was prepared. This overview contained three major systems of the APS STAR power plant:

1. Ocotillo Photovoltaic system 1 (OPV-1) (Figure 6);
2. Ocotillo Photovoltaic system 2 (OPV-2) (Figure 7)
3. Fixed Tilt System (South facing at 33° latitude tilt) (Figure 8)

See Table 3.1 to understand the nomenclature used to denote modules mentioned in the plant level and string level diagrams. The names of the manufacturers have not been disclosed.

Table 3.1 Module designation and count for the APS STAR power plant

Model designation and module count								
Array	Model A18	Model A13	Model B	Model C12	Model C4	Model D	Model E	Model F
Size	9 kW	11.6 kW	81.9 kW	51.3 kW	51.3 kW	12 kW	8.8 kW	14.4 kW
#Modules (1-axis)	168		1155	176	40	48	50	120
#Modules (Lat. Tilt)		216	-		-	-	-	-
#Modules (String)	3	21	21	8	8	8	12	23
String Voltage (Voc)	65	455	455	505	505	485	532	483
Years Fielded	18	13.3	13.3	11.7	3-4	11.7	11.7	11.7
Structure	Framed	Framed	Frameless	Framed	Framed	Framed	Framed	Framed

The modules are designated as A through F based on their models. Model A and C have been further segregated based on years fielded. APS records and staff were the main sources of this information. In addition, this ensured that the nomenclature remained consistent with a similar study done at the STAR center in 2010 [20]. Figure 3.4 depicts the modules at the APS STAR site.

Figure 3.4 (a) Picture of the three tested systems at APS STAR

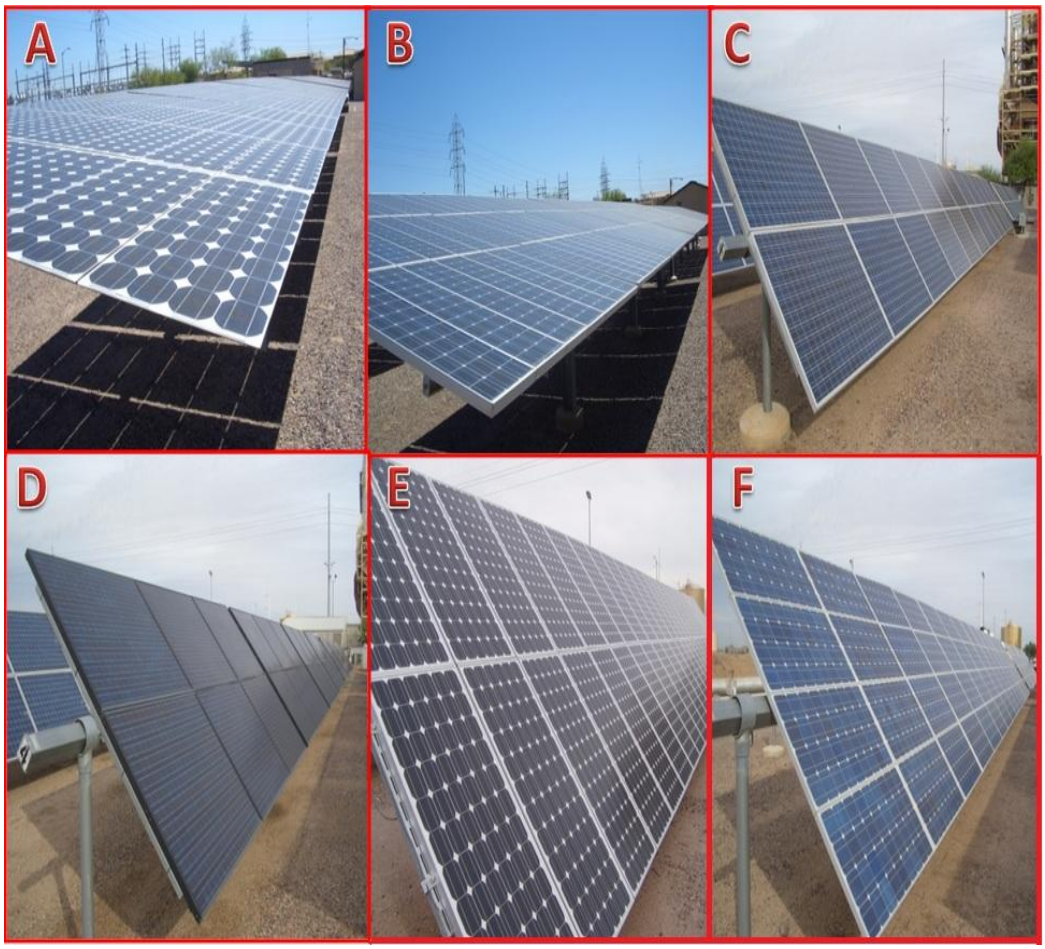

Figure 3.4 (b) Pictures of the modules at APS STAR [20]

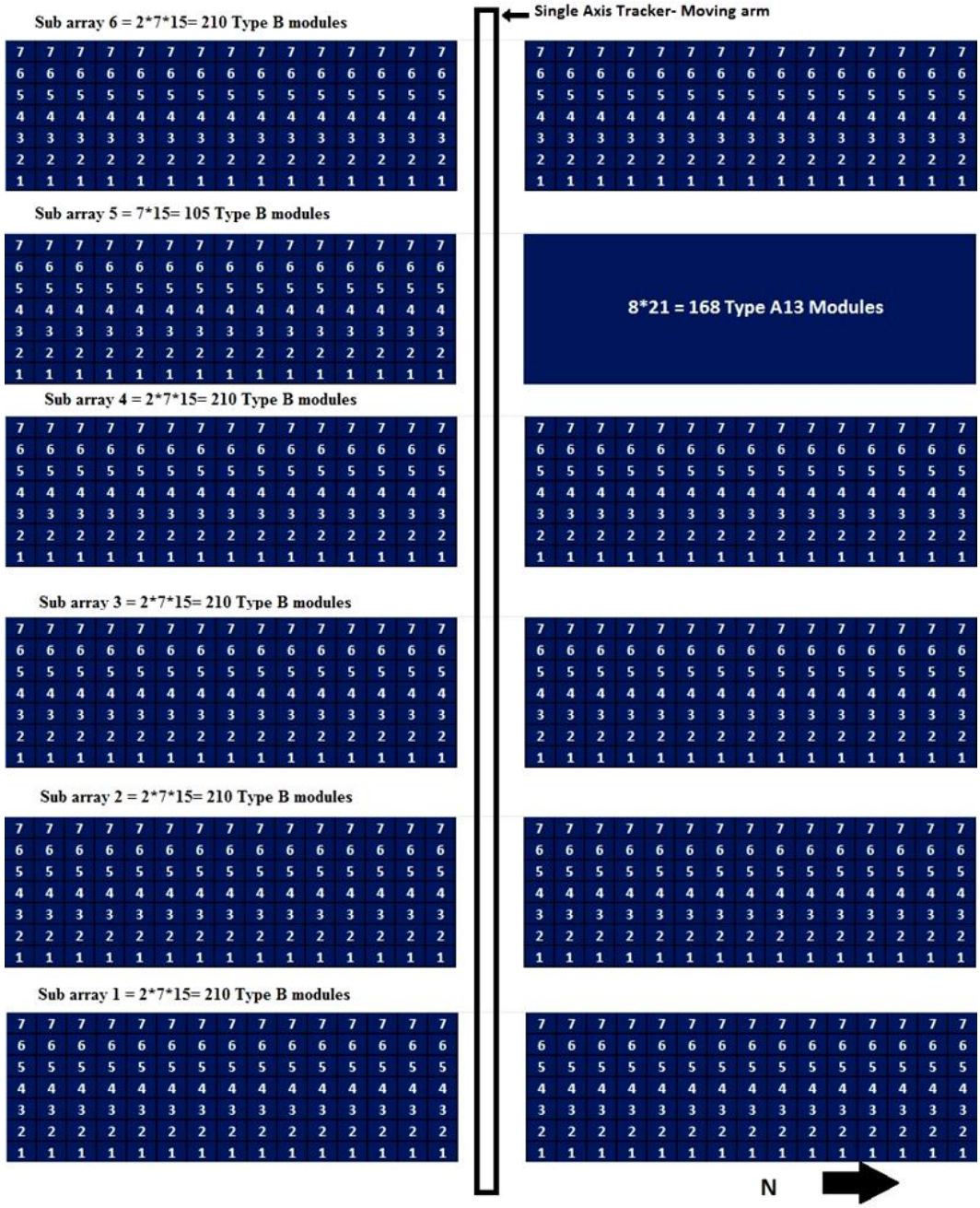

Figure 3.5 Array Layout for the 78.5 kW single Axis Tracker (OPV-1)

Figure 3.5 refers to OPV-1, which has a total of 1,323 modules, 1,155 of which are type B modules. Only 216 modules are type A13 modules. Both these module banks are 13.3 years old. Each row has two wings, namely, North wing and South Wing. The North wing has been referred to as the "right wing," and the

South wing has been called the "left wing" throughout the nomenclature of data collection and analysis.

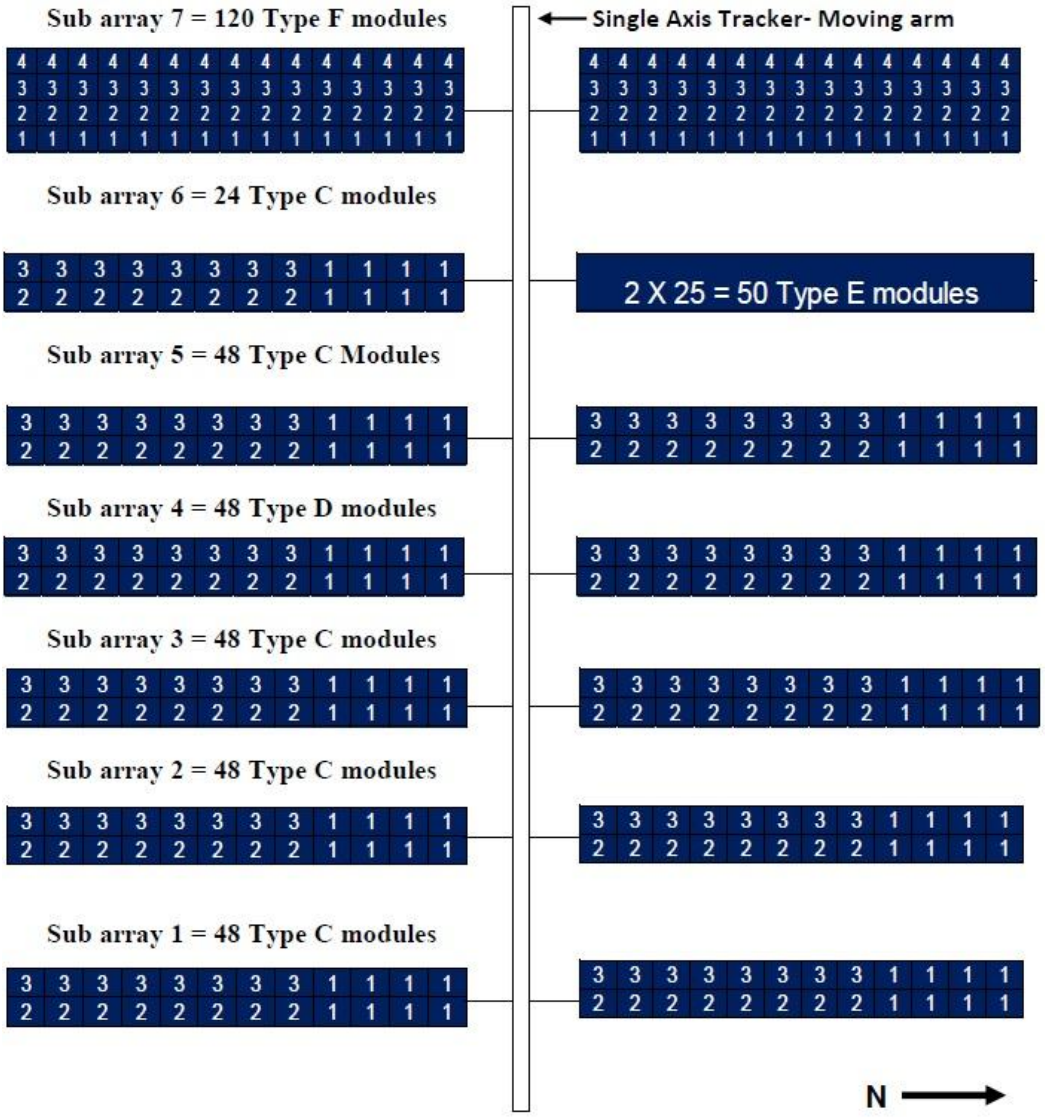

Figure 3.6 Array Layout for the 115 kW single Axis Tracker (OPV-2)

The array layout for OPV-2 is shown in Figure 3.6. It contained a total of 216 type C modules, 48 type D modules, 50 type E modules, and 120 type F modules. Figure 3.7 provides the array layout for the south facing fixed tilt array, which contained 216 type A18 modules.

Bank 1	3*6= 18 Type A18 Modules	3*6= 18 Type A18 Modules
Bank 2	3*6= 18 Type A18 Modules	3*6= 18 Type A18 Modules
Bank 3	3*6= 18 Type A18 Modules	3*6= 18 Type A18 Modules
Bank 4	3*6= 18 Type A18 Modules	3*6= 18 Type A18 Modules
Bank 5	3*6= 18 Type A18 Modules	3*6= 18 Type A18 Modules
Bank 6	3*6= 18 Type A18 Modules	3*6= 18 Type A18 Modules

Figure 3.7 Fixed Tilt array -11.6 kW (South facing)

3.3.2 String Circuit

For a detailed analysis of the power plant at the string level, string circuit diagrams were prepared for each individual string. The grounding technique for each system and module type was noted to determine the biasing of the string circuit. The position of each module in the respective string was calculated based on actual wiring existing at the plant.

As seen in Figure 3.8, the negative end of each string in OPV-1 was centrally grounded, which means that the string was positively biased. Thus, the module nearest to the ground potential is considered as the first module (module 1) in the string; it has the lowest level of potential impressed across it. However, the module farthest from the ground potential is considered as the last module (module 21) in the respective string; it has the highest level of potential impressed across it. The same setup runs across five other rows in OPV-2 that contains the same number of modules (except row 5 right).

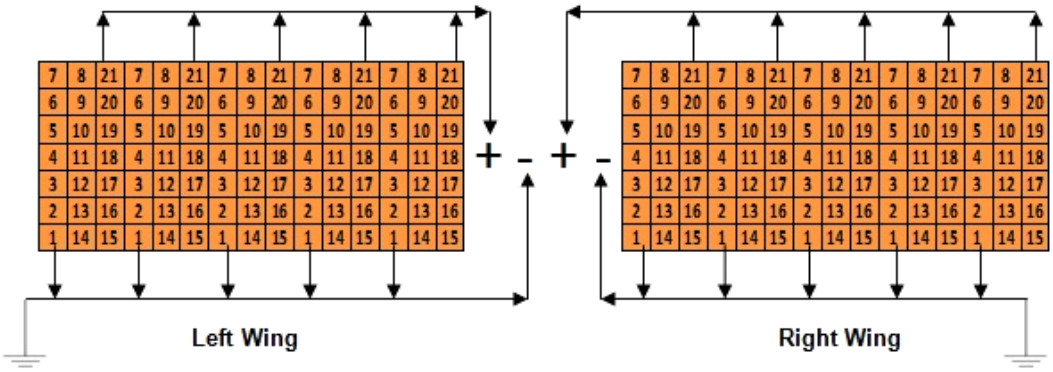

Figure 3.8 Series Connection Diagram for type B modules on OPV-1

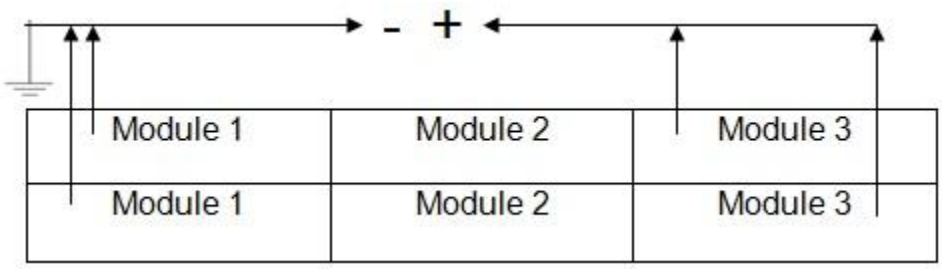

Figure 3.9 Series Connection Diagram for type A18 modules on fixed tilt system

Figure 3.9 represents the circuit diagram of the type A modules located on the fixed tilt PV array. Module one is connected to the negative (grounded) end of the string. Modules two and three are in series with Module 1. The string ends at Module three, which is connected to the positive end on the junction box. Thus, Module three is the last module in this positively biased string. The connection scheme is same for the bottom row, and the same setup runs across 36 such banks.

The series circuit diagram for type C and D is exactly the same and is explained in Figure 3.10. A total of 24 modules are divided into three strings of eight modules each. The numbers one through eight denotes the proximity of a module from the ground. Therefore, the negative end of module one is grounded.

Module eight is the last module in each string, making the whole circuit a positively biased string.

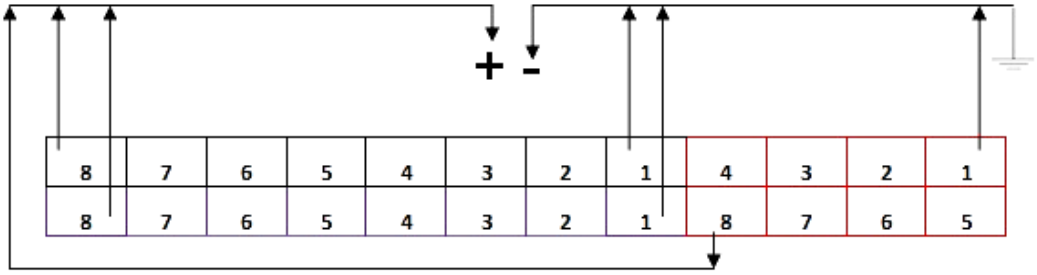

Figure 3.10 Series Connection Diagram for type C and D modules on OPV-2

Row six right in the OPV-2 system consists of 48 type E modules. A total of four strings are in this module scheme, and each string consists of 12 modules in series. The first module is negative (grounded) and the last (12) module forms the end of the string. The twelfth module forms the positive end of the string, making the circuit positively biased. Figure 3.11 depicts the string circuit of one of the strings in row six right of OPV-2

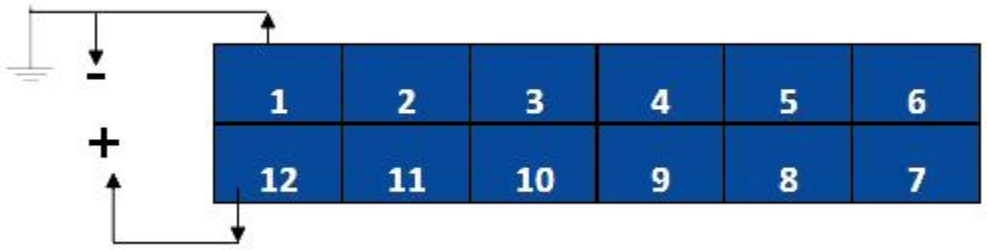

Figure 3.11 Series connection Diagram for type E modules on OPV-2

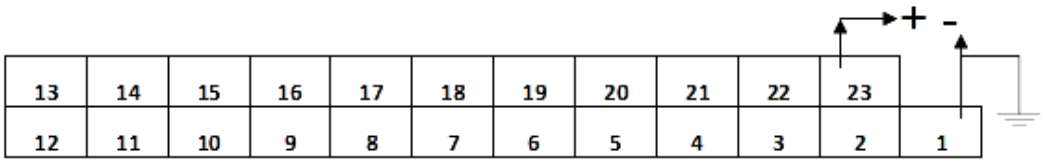

Figure 3.12 Series Connection Diagram type F modules on OPV-2

The last rows, namely rows seven right and seven left, on OPV-2 consist of the of type F modules. A total of 92 modules are a part of the system. Four strings are in row seven, and each string consists of 23 modules. Figure 3.12 explains the circuit connection for row seven. Module one connects to the negative end of the circuit and is grounded. Module 23 is the last module and is connected to the positive end in the circuit. All four strings are connected in a similar fashion. This circuit is also positively biased with the negative end grounded.

CHAPTER 4

RESULTS & DISCUSSION

4.1 Overall Power Degradation

Individual I-V curve data collected from approximately 1,900 modules provided some interesting results. Out of a total of eight models existing at the STAR center, five (~60%) models do not seem to meet the common 20/20 warranty (20 % degradation for 20 years). Referring to the overall number, about 1,604 of the 1,855 modules measured failed to meet the common 20/20 warranty expectation. This represents approximately 86% of the total number of modules.

The degradation percentage given in Figure 4.1 is the average of the total degradation of a respective module. The normalized power was compared to the nameplate rating, and power degradation percentage was calculated. As can be clearly seen, the power degradation of module A18 is the highest at 43.95%. It has been fielded for 18 years and is the oldest in the lot. Model A13, which has fielded for 13.3 years, has degraded by 32.85%. Model A18 and A13 are similar in construction; therefore, one can determine that both the age and construction has resulted in the degradation of these modules. The average overall degradation for model B is 20.34%, and it also fails the warranty expectation. Model B is the highest count module, so it dominates the overall failure percentage of the plant.

Models C1, D, and E, aged 11.7 years, are the only modules whose average degradation rate is projected to satisfy the warranty expectations; assuming a linear degradation, their average degradation is calculated to be less than 20% in 20 years. If fielded for more than 20 years, it can be estimated that they will make it through with the common 20/20 power delivery warranty. Model F has behaved

randomly with respect to its age bracket. The average degradation of model F over a period of 11.7 years was calculated to be 16.43%.Thus, the rate of degradation for this module is high. Model C4 has the strangest behavior observed among all modules. This model is a set of replaced modules provided by the manufacturer after some modules failed to perform in accordance to the warranty clause. These modules exhibited a very high overall degradation percentage and the highest degradation rate.

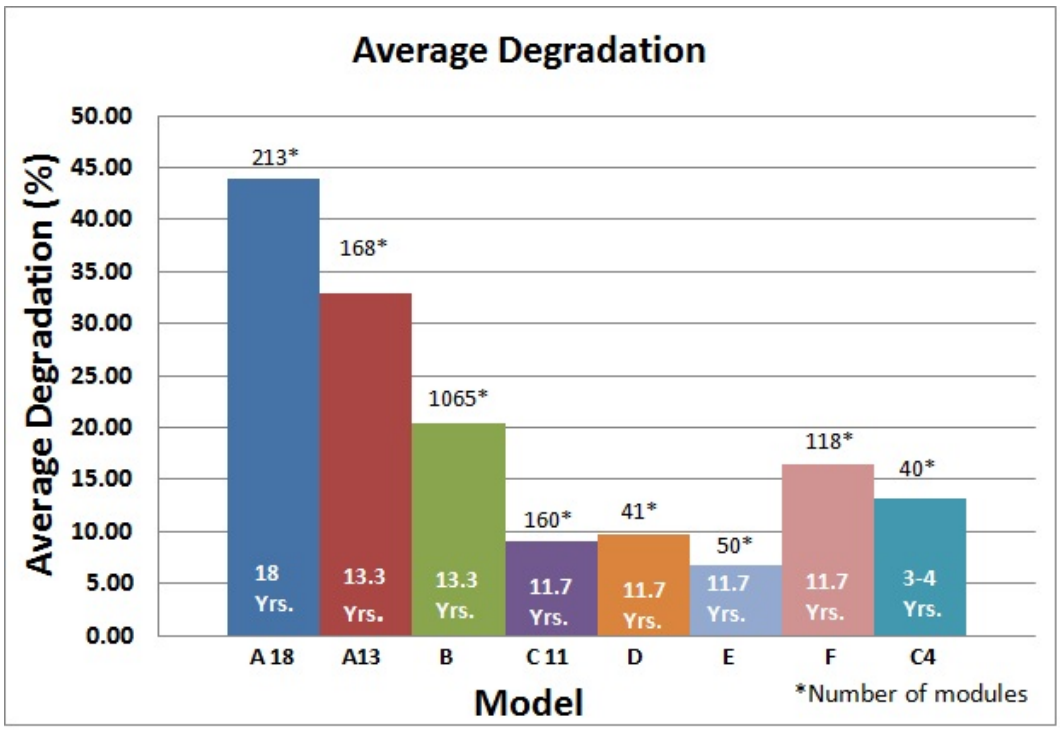

Figure 4.1 Power degradation (average) of all modules

The degradation rates of all the modules have been calculated by dividing their average overall degradation percentage with the number of years fielded. The average annual degradation rates for all module types are plotted in Figure 4.2.

The modules with higher percentage degradation (A18 and A13) represent the same manufacturing technology. They have annual degradation rates of 2.44% and 2.47%, respectively.

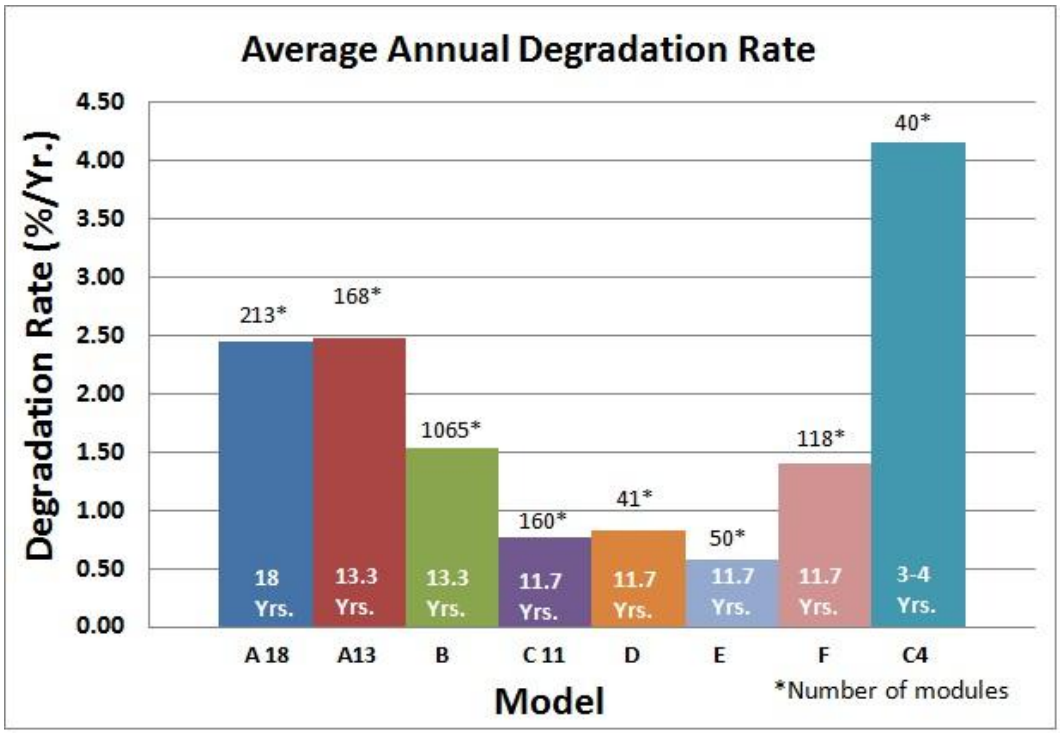

Figure 4.2 Rate of degradation/year (average) of all modules

Figure 4.2 shows the rate of degradation for module C4 to be the highest. As mentioned earlier, this model represents a set of replacement modules. Their poor performance might be attributed to some manufacturing issues of replacement modules that were produced by the new purchaser of an old company several years (>9 years) after the production of original modules.

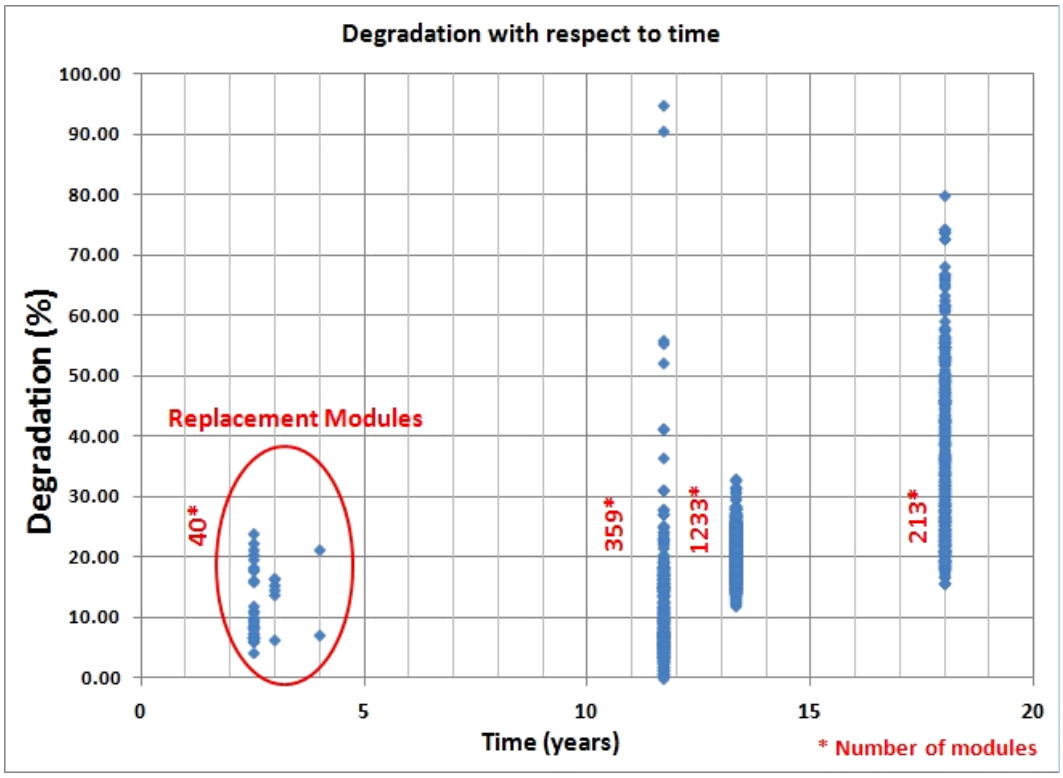

Figure 4.3 Degradation versus time plot

Figure 4.3 shows the behavior of the modules at APS STAR with the passage of time. Clearly, as the number of years fielded by the modules increases, the degradation increases. The replaced modules again behave unusually in this plot.

Table 4.1 provides the detailed degradation rate (percentage) and annual degradation rates for all the tested modules in this project at the STAR center. The annual degradation rates for the power plant vary from 0.57% to 2.47%.The degradation percentage and annual rates are slightly different from those reported in 2010 (0.99% to 1.92%), a year before this study [20], which is due to the difference in sample size in these studies. A total of 60 healthy (free from cosmetic defects) modules were tested in 2010 [20]. The sample size of 1,900

modules studied in 2011 surpasses these numbers by far and, therefore, can be considered more accurate representation of the power plant.

Table 4.1 Degradation rates for all modules

Degradation rates by Model						
Model of Module	Years Fielded	% Degradation (2011)	% Degradation/Year (2011)	% Degradation/ Year (2010)	No. Of modules studied (2010)	No. Of modules studied (2011)
A 18	18	-43.95%	-2.44%	N.A	0	213
A 13	13.3	-32.85%	-2.47%	-1.92%	10	168
B	13.3	-20.34%	-1.53%	-1.86%	10	1065
C 12	11.7	-9.02%	-0.77%	-1.34%	10	160
C 4	11.7	-13.13%	-4.14%	N.A	0	40
D	11.7	-9.69%	-0.83%	-0.99%	10	41
E	11.7	-6.68%	-0.57%	-0.93%	10	50
F	11.7	-16.43%	-1.40%	-1.68%	10	118

Table 4.2 Comparison of degradation rates of 2011 with the rates in 2010

Degradation rates comparison 2010 to 2011					
Model of Module	% Degradation/Year (2011)	% Degradation/Year Unhealthy (2010)	% Difference between 2011 and 2010 Unhealthy	% Degradation/Year healthy (2010)	% Difference between 2011 and 2010 healthy
A 18	-2.44%	N.A	N.A	-1.92%	-0.52%
A 13	-2.47%	N.A	N.A	N.A	N.A
B	-1.53%	-2.95%	1.42%	-1.86%	0.33%
C 12	-0.77%	-1.90%	1.13%	-1.34%	0.57%
C 4	-4.14%	N.A	N.A	N.A	N.A
D	-0.83%	-1.25%	0.42%	-0.99%	0.16%
E	-0.57%	N.A	N.A	-0.93%	0.36%
F	-1.40%	-4.96%	3.56%	-1.68%	0.28%

Table 4.2 compares the new degradation rates with those reported in 2010 based on their functionality (Healthy/Unhealthy). Clearly, the degradation rates reported in 2010 for both healthy (visually free from failures and defects) and unhealthy (visual cosmetic defects/hotspots) modules were higher than the more recent results. This difference can be attributed to the lower sample size used in

2010. Because some categories were not subdivided in 2010, their degradation rates have not been reported in this table. Only one category of reported degradation rates in 2011 shows a higher degradation rate than the 2010 healthy modules. This may be attributed to the higher performance of a certain section of modules from the array, which could have been randomly selected for measurement.

4.2 Potential Induced Degradation

The effect of voltage (PID) on the degradation of modules connected in a string has been examined extensively. Three factors favored the study of PID at the STAR center as follows:

1. Series connection of PV modules to obtain higher voltage levels in a power plant setting;
2. Positively biased strings throughout the power plant due to centralized negative grounding in the inverter; and
3. Hot and dry climatic conditions of Arizona.

The detailed string level circuits were prepared for the whole system and the overall percentage power degradation of each module in the string was plotted in a scatter plot. A trend line was drawn in each of the plots to investigate a constant trend in the degradation of modules with respect to their position (proximity to ground) in the string.

Three random strings from OPV-1 are presented in Figure 4.4, Figure 4.5, and Figure 4.6. The string plot in Figure 4.6 suggests that the last module in a positively biased string experiences 20% higher degradation than does the first (grounded) module. By contrast, Figure 4.5 indicates 30% higher degradation at the negative (grounded) end of the string. In the same context, we can deduce

from Figure 4.6 a similar degradation at both ends of the string. These three different trends seen throughout OPV-1 clearly demonstrate the absence of PID in OPV-1.

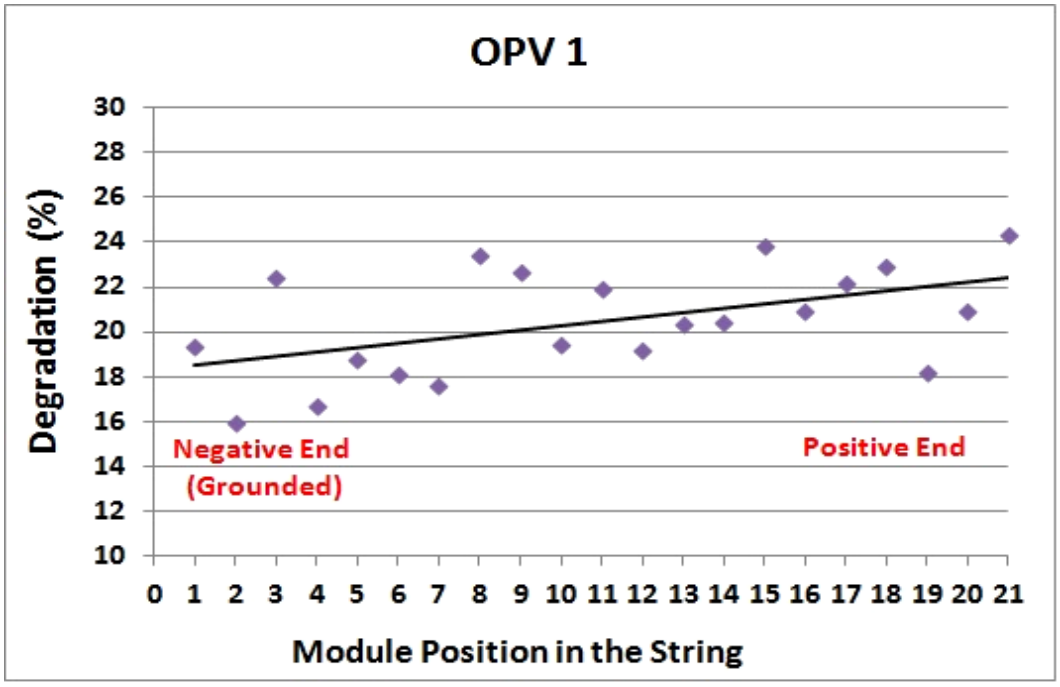

Figure 4.4 Higher degradation percentage at positive end of string (OPV-1)

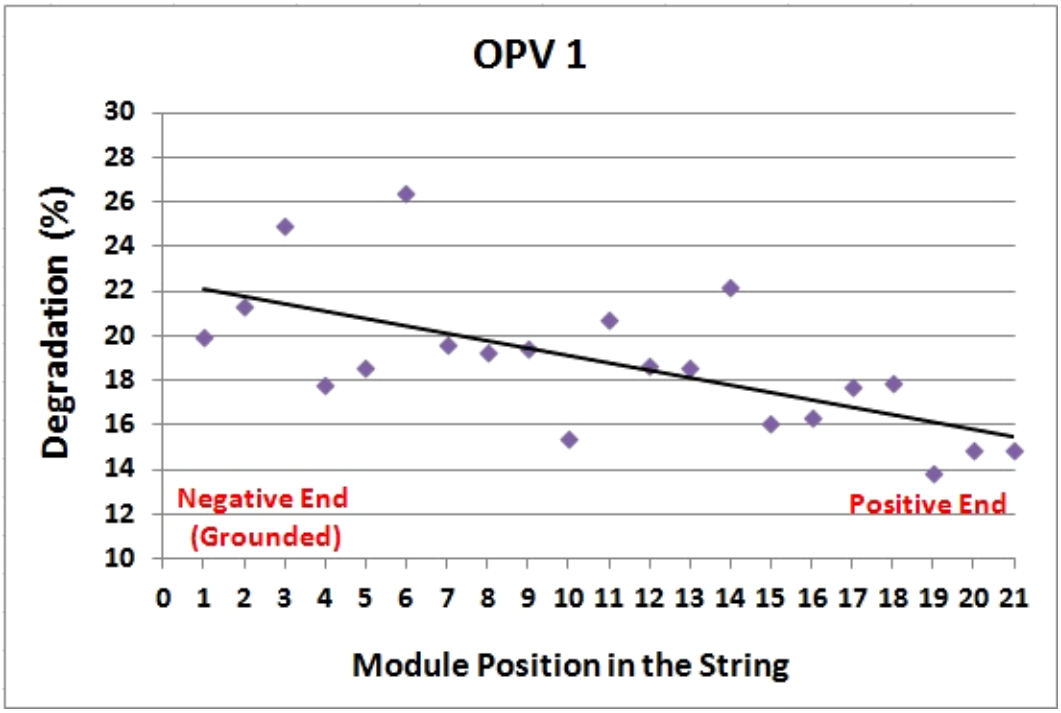

Figure 4.5 Higher degradation percentage at negative end of string (OPV-1)

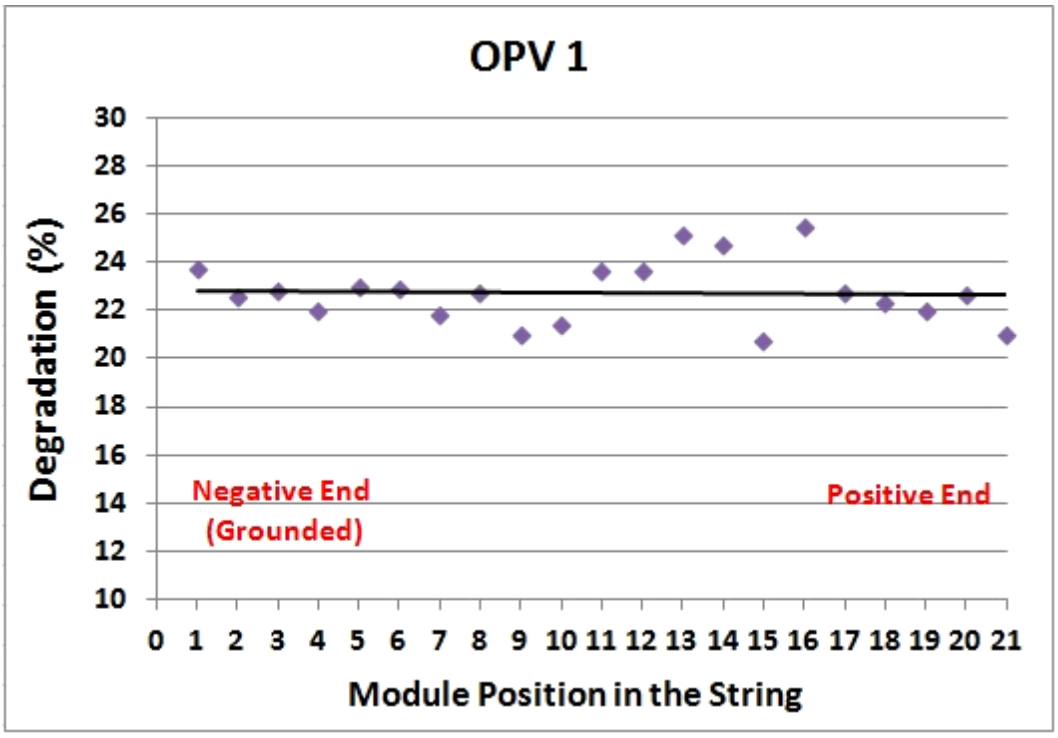

Figure 4.6 Similar degradation percentage at both ends of string (OPV-1)

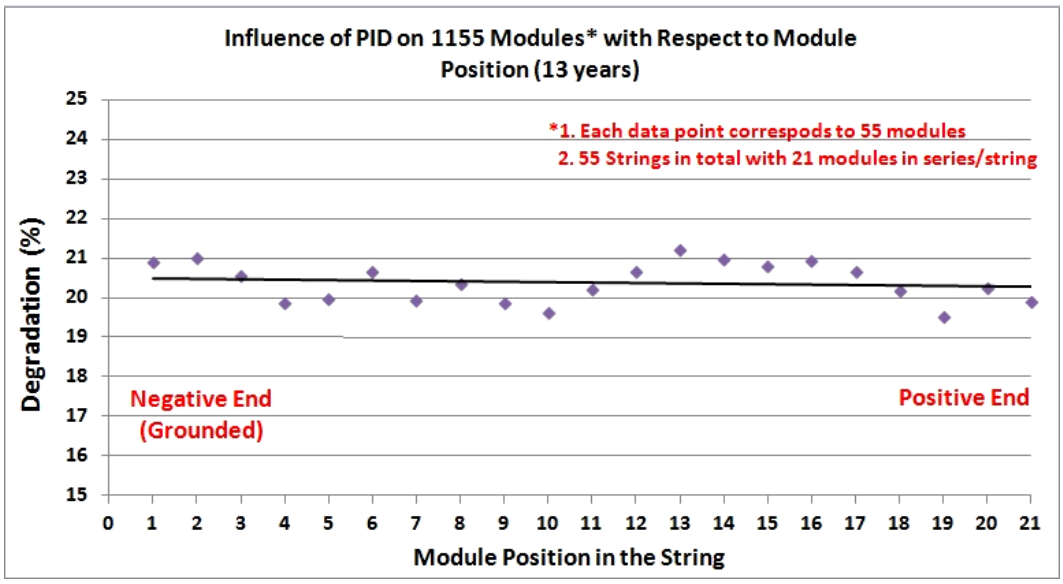

Figure 4.7 Influence of PID on 1,155 modules with respect to module position in the string

Figure 4.7 summarizes OPV-1 in one plot; all the modules (55 in total) at the same position throughout OPV-1 have been plotted together. Model A13, located in row 5 right of OPV-1, has been excluded from this plot due to unavailable circuit structure. Therefore, all 1,155 modules belong to model B and have fielded for 13.3 years. Measured data for module B was available for 1,065 of these modules. The power for 90 missing modules was adjusted by using average string power and following the same trend as the string.

The total number of strings exhibiting an increasing slope, decreasing slope and constant slope of power degradation with respect to position in a string were 18, 24 and 13 respectively. Thus, no real trend on an average is seen in OPV-1. Therefore, the PID effect is considered to be absent in OPV-1; however, a detailed statistical analysis of all the strings needs to be performed to strengthen this conclusion.

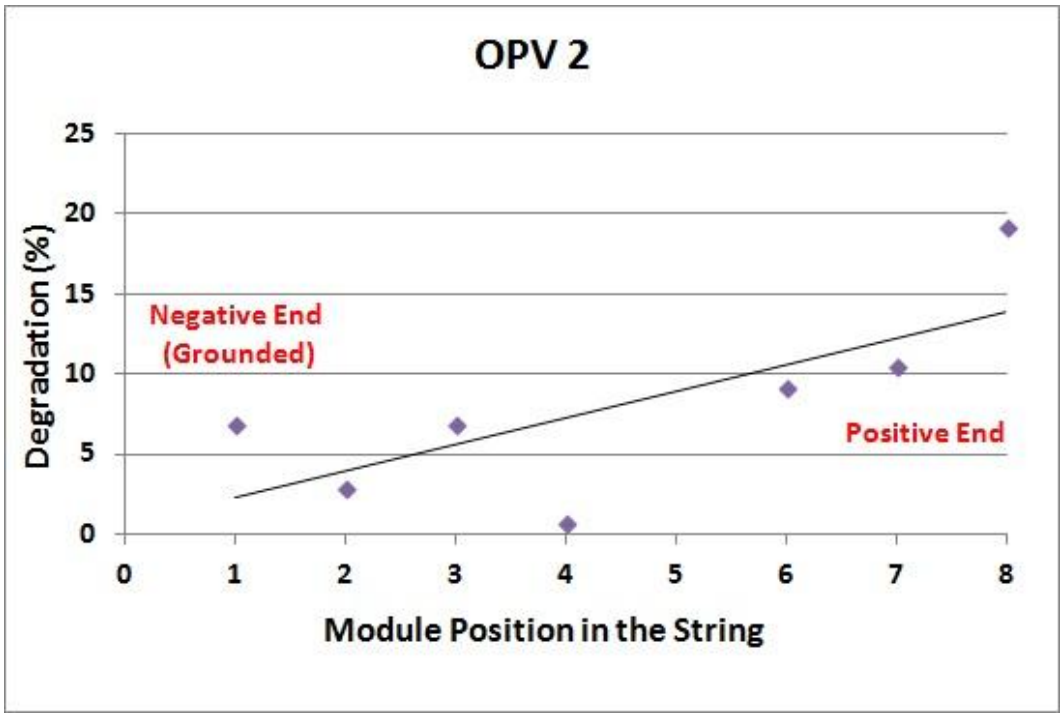

Figure 4.8 Higher degradation percentage at positive end of string (OPV-2)

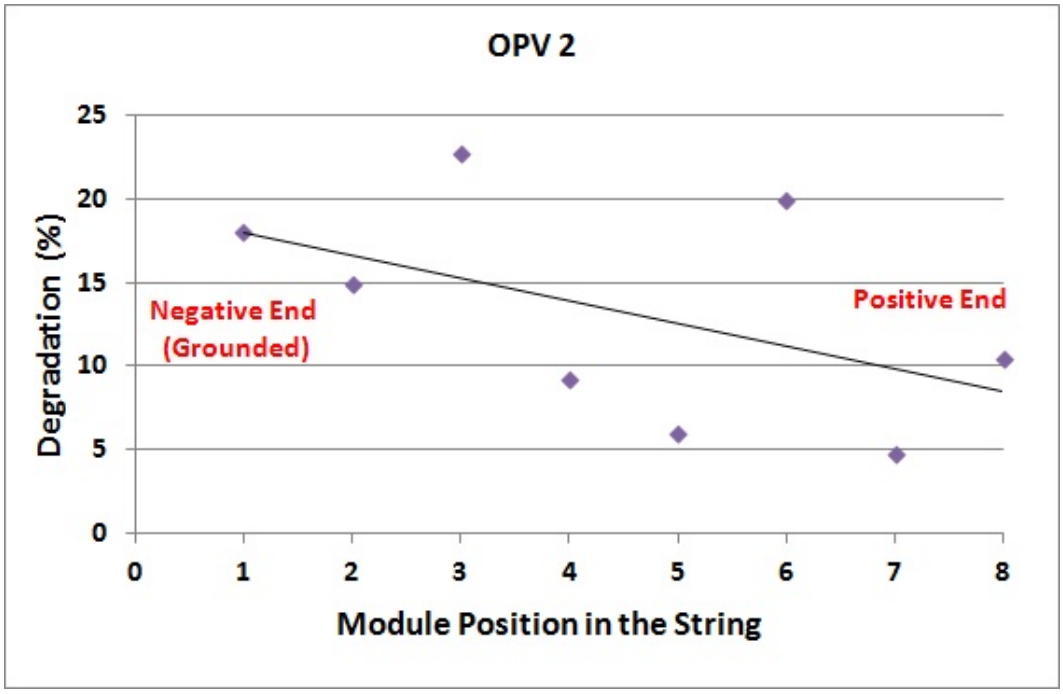

Figure 4.9 Higher degradation percentage at negative end of string (OPV-2)

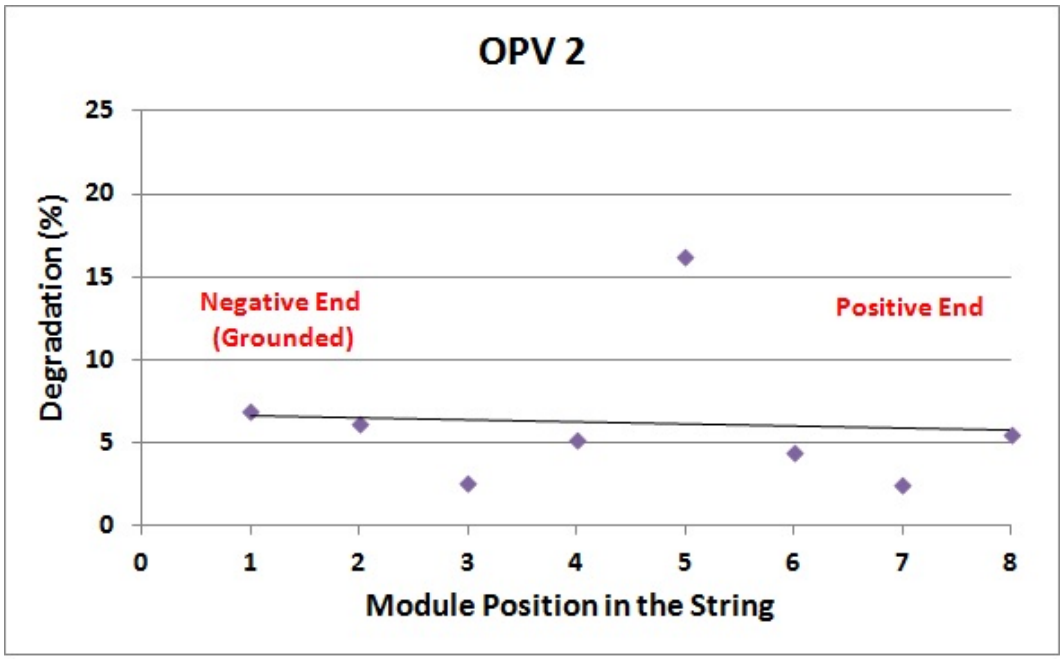

Figure 4.10 Similar degradation percentage at both ends of string (OPV-2)

Further analysis to investigate the PID effect was conducted on model C modules in OPV-2. A total of 216 modules in 27 strings were measured and plotted according to their string circuit. From Figure 4.8, Figure 4.9, and Figure 4.10, we can see random module performance degradation. The voltage seems to have no constant effect on the performance degradation of any of the modules with respect to positioning in the string in a positive biased circuit. The total number of strings exhibiting an increasing slope, decreasing slope and constant slope of power degradation with respect to position in a string were 13, 9 and 4 respectively.

Figure 4.11 depicts the average plot of type C modules in OPV-2 according to the string position of all 27 modules across strings of eight. OPV-2 shows no consistent trend, and random trends mark the array in OPV-2. This includes module D, E, and F. Their plots are not discussed because they have very few strings. Because no effect is seen, one can infer that positively biased OPV-2

has no PID effect. Again, a detailed statistical analysis of all the strings needs to be performed to strengthen this conclusion.

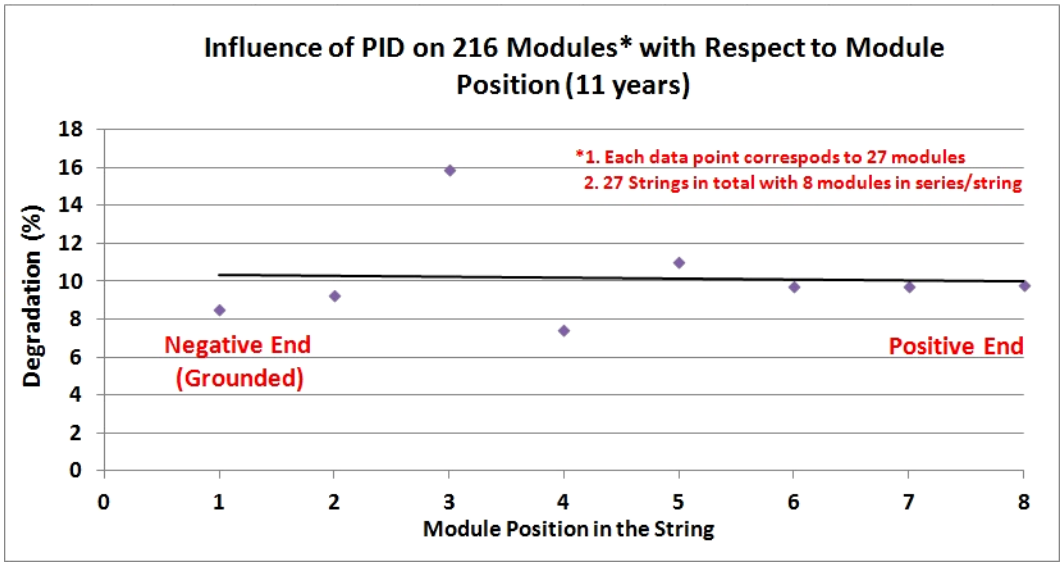

Figure 4.11 Effect of PID on 200 modules with respect to module position in the string (OPV-2)

To investigate the PID effect on a positively biased system as a factor of time, the same analysis has been performed on the fixed tilt system containing model A18. These 18-year-old modules have the highest amount of degradation at the STAR center.

Although there are only three modules per string, they are plotted according to their connection diagram. Because these modules were used to support a hybrid system with nominal voltage of 48 V, they have a lower number of modules in series.

Figure 4.12, Figure 4.13, and Figure 4.14 clearly point out the absence of PID in the fixed tilt system as well. All the strings in the fixed tilt system show random performance degradation trends.

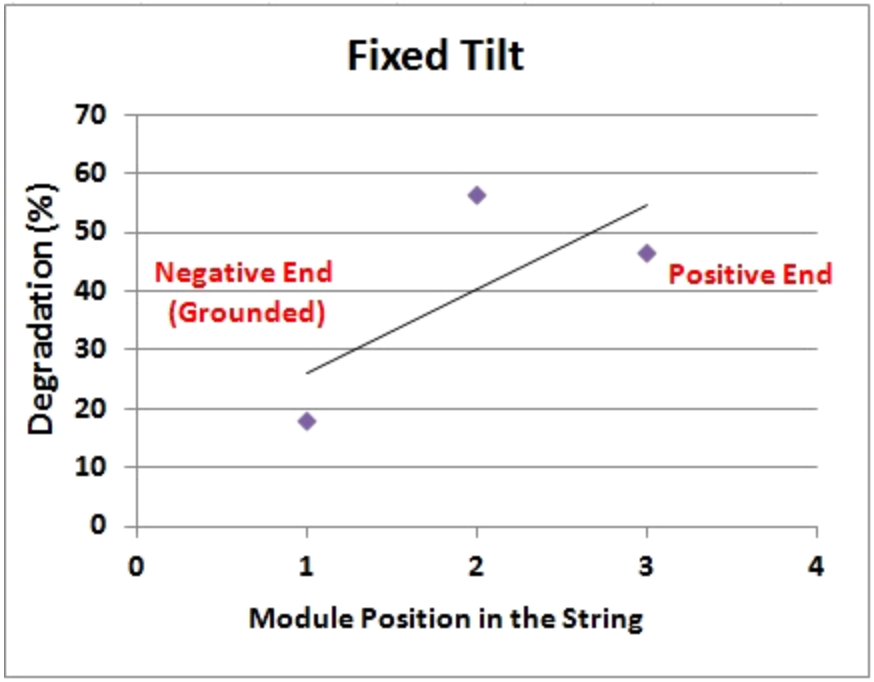

Figure 4.12 Higher degradation at the positive end of the string (fixed tilt)

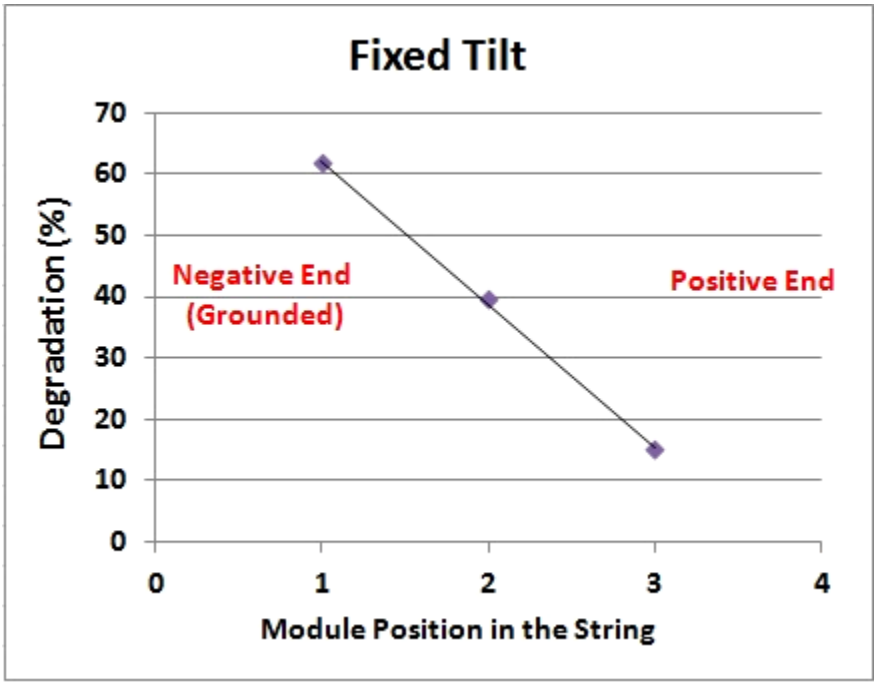

Figure 4.13 Higher degradation at the negative end of the string (fixed tilt)

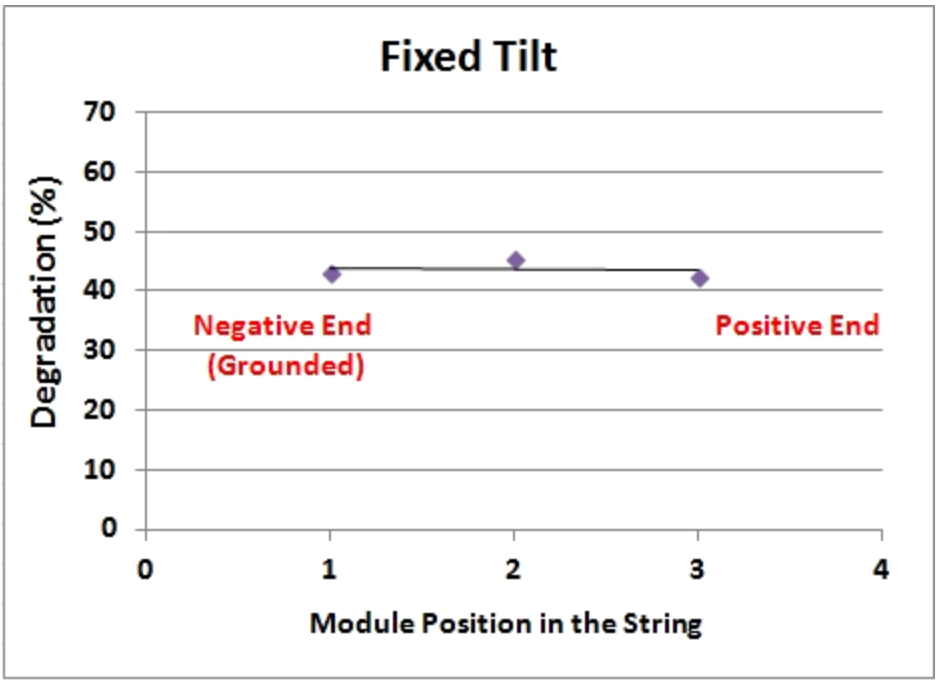

Figure 4.14 Similar degradation percentage at both ends (fixed tilt)

4.3 Module Mismatch at the String Level

The individual I-V curve data was used to calculate the mismatch effect at the string level. The STC power of each module was plotted in the string diagrams, and further analysis produced some interesting findings. The formula used for calculating the power drop due to mismatch is as follows:

$$\text{Module mismatch drop of a string} = \frac{\text{(Sum of individual module power - String Power)}}{\text{(Sum of individual module power)}}$$

$$\text{Module mismatch drop of a string} = \frac{P_{SUM} - P_{STRING}}{P_{SUM}}$$

Upon finding the module mismatch of all the strings, they were plotted according to their models. Figure 4.15 plots power drop due to mismatch in the 55 strings. A total of 1,155 modules were connected across 55 strings, with 21 modules in series for each string. The I-V data for approximately 100 modules out of 1,155

went missing or became corrupted. The missing module power was then calculated as an average of the remaining modules, following the right trend. As shown in Figure .15, the average power drop in model B (13 years) due to mismatch in the string was 21.86%.

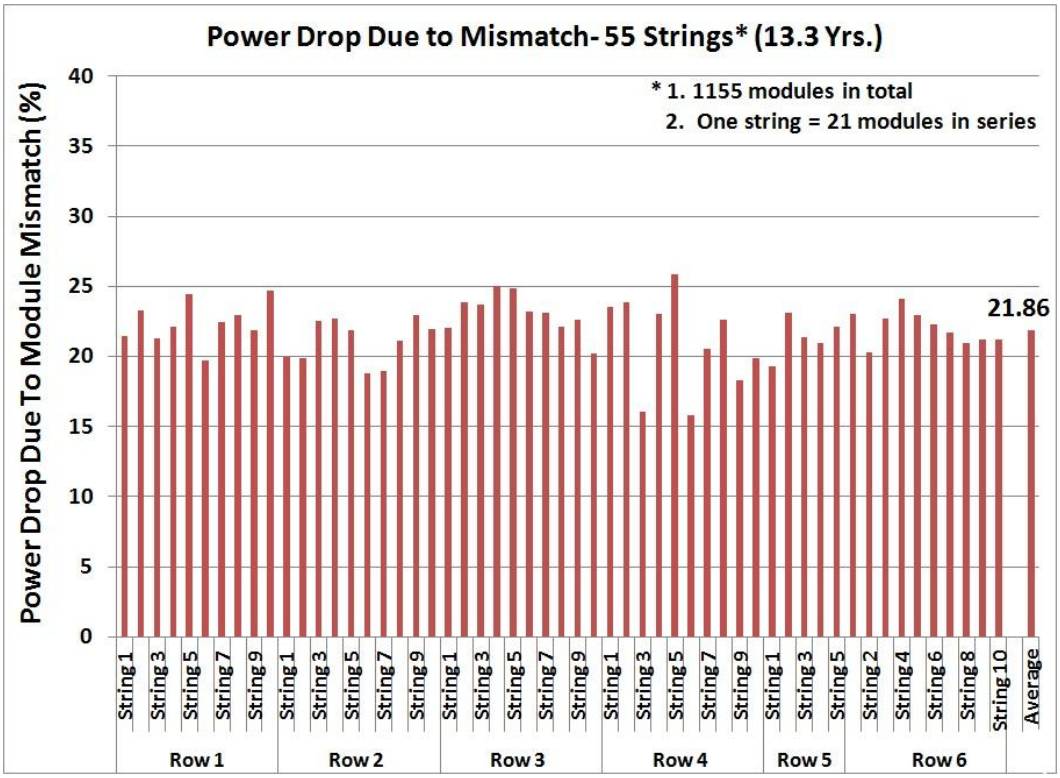

Figure 4.15 Power drop due to mismatch in 55 strings (1155 modules), Model B

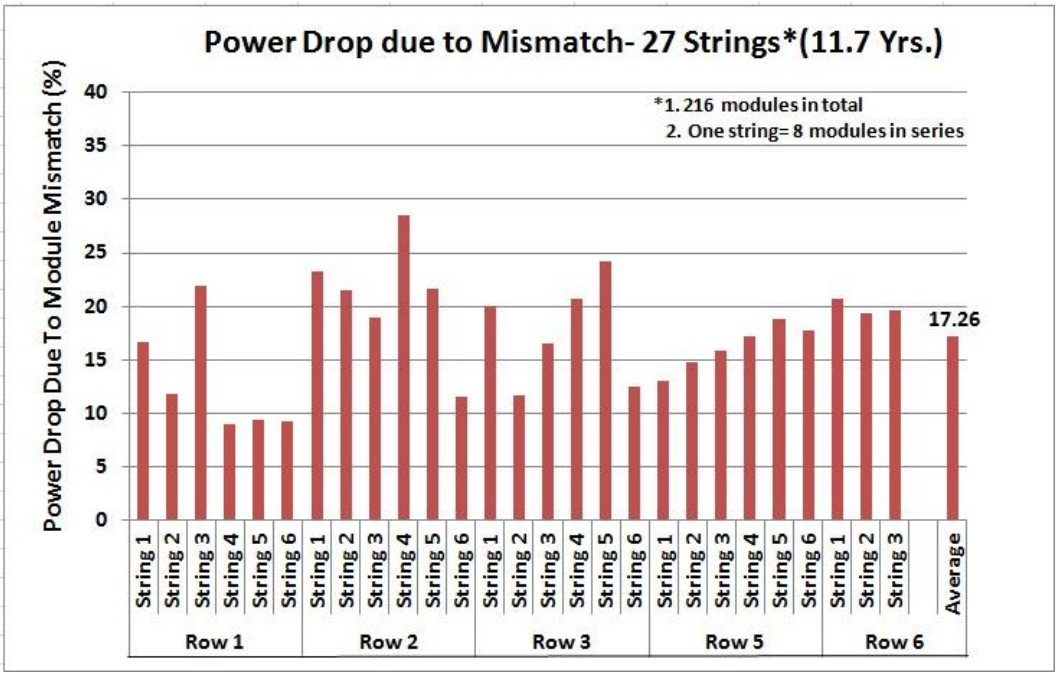

Figure 4.16 Power drop due to mismatch in 27 strings (216 modules), Model C

Figure 4.16 depicts the drop of power in model C. A total of 216 modules connected in a series of eight modules made up 27 strings; they are part of OPV-2. The average power drop due to module mismatch for model C modules (11.7 years old) was 17.26%, which is less than the power drop in modules 13 years old. The notable feature here is the variation of 8 to 25% in the amount of power drop. The average module mismatch power drop for model D is 16.94%, which is slightly lower than model C. Model D consists of 48 modules, spread across six strings of eight modules (in series) each.

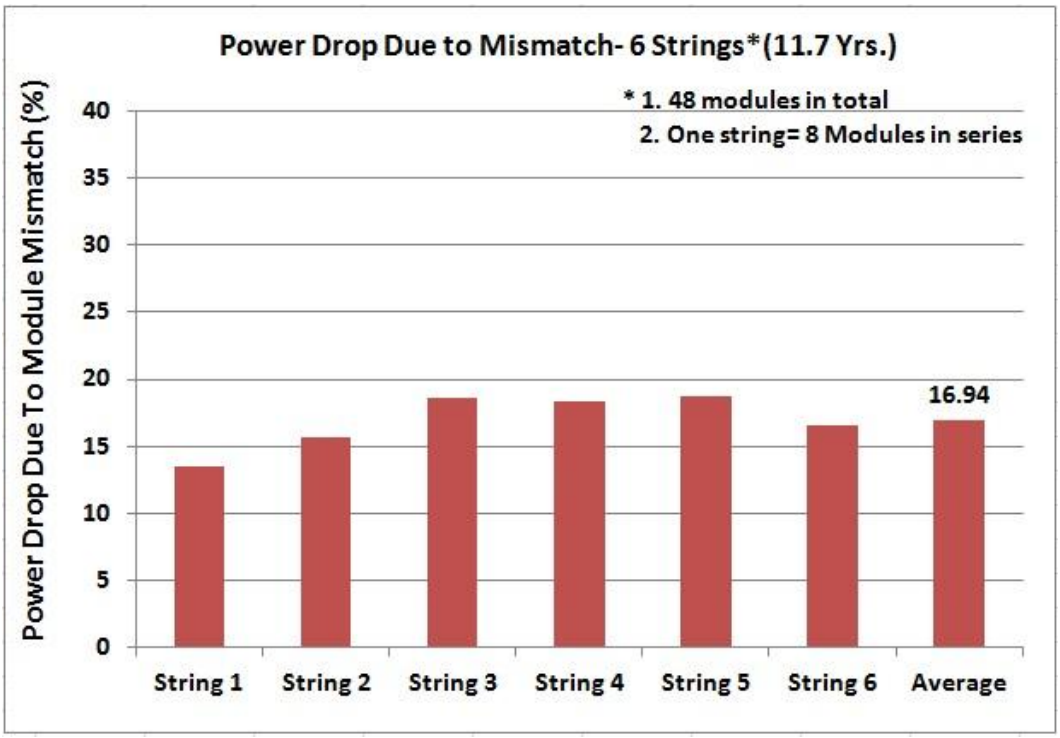

Figure 4.17 Power lost due to mismatch in six strings (48 modules), Model D

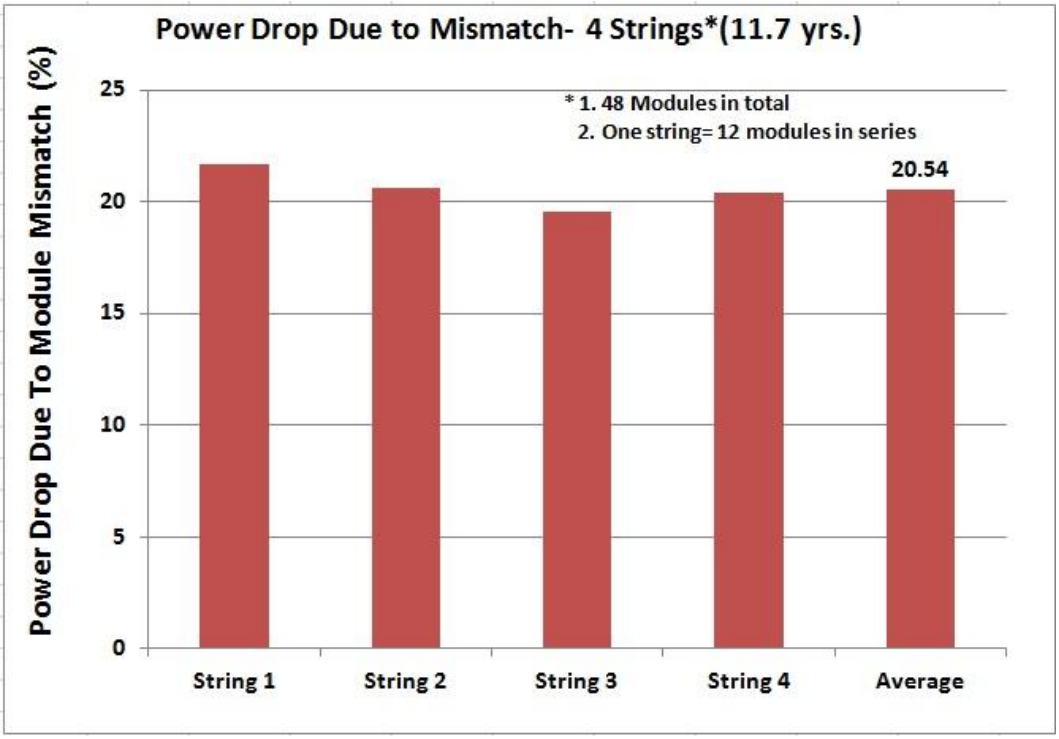

Figure 4.18 Power drop due to mismatch in four strings (48 modules), Model E

Figure 4.18 plots the drop of power in model E due to mismatch at the string level. Little variation occurs in the power drop in the four strings containing 12 modules each. The average power drop for this category comes out to be 20.54%. The higher average can be attributed to a higher number of modules in the string, which may also be an issue of increased series resistance.

As seen in Figure 4.19, model F contains four strings, and each string contains 23 modules in series. As depicted earlier, the power degradation of this type is higher when compared to modules of the same age. Here, the average drop in power is 24.57%, which is more than the 13-year-old module (model A) that contained 21 modules in series. Clearly, both the age of a module and the number of modules in that string have an impact on the drop of string power in series connected modules. This phenomenon becomes further aggravated when random degradation of modules connected in a string occurs due to material/design/ageing issues.

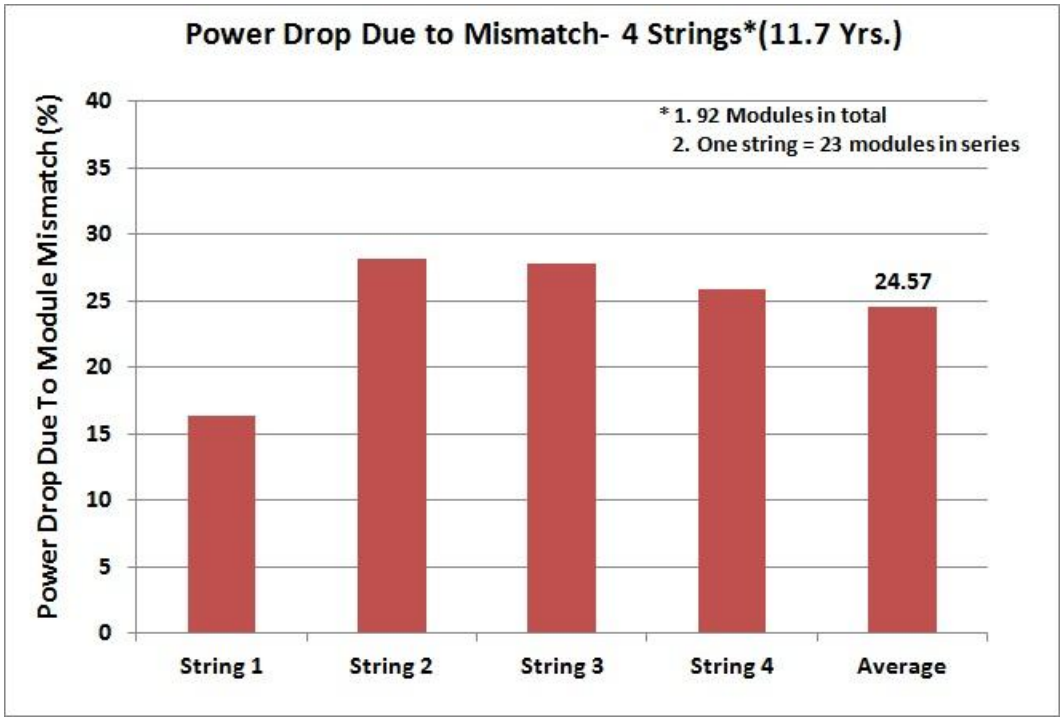

Figure 4.19 Power drop due to mismatch in four strings (92modules), Model F

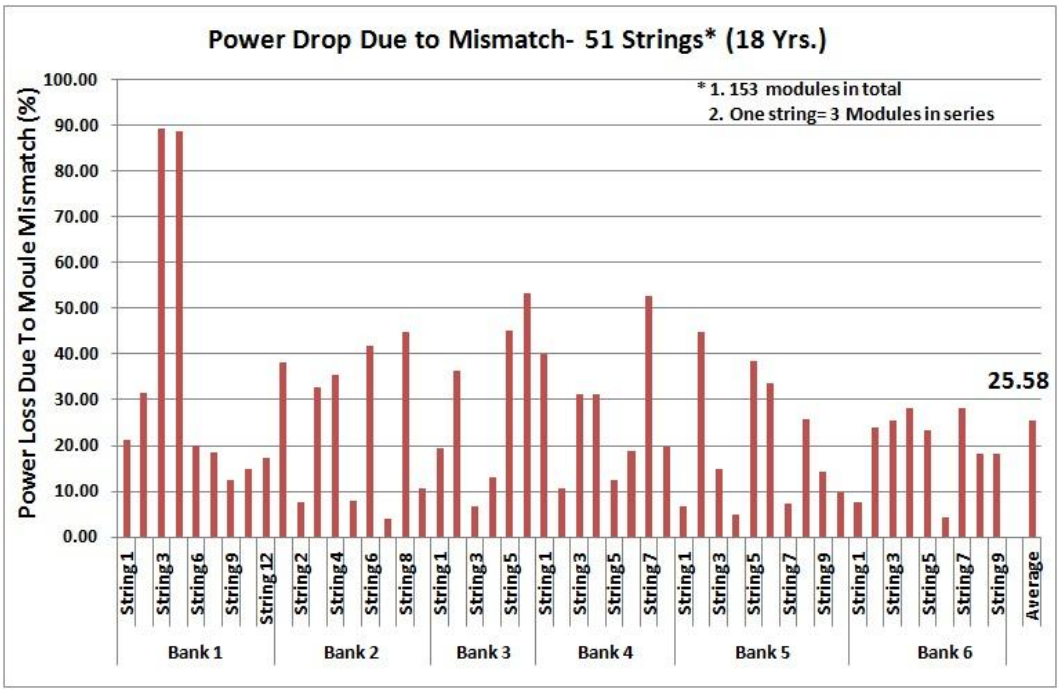

Figure 4.20 Power drop due to mismatch in 51 strings (103 modules)

The last model to be discussed for module mismatch power drop is type A18. Figure 4.20 represents the 51 strings of type A18 modules. Being the oldest modules in the plant, the performance degradation observed for this type was the highest. String three and four in bank 1 exhibit highest mismatch because of extremely low voltage and extremely low voltage/low current in those strings. The mismatch issue can be seen to be the highest in this case. About 21 strings of A18 were not included in this study because of missing/corrupted data. Due to a lesser number of modules in a string (three) and random performance degradation among stringed modules in the fixed tilt system, no approximation was done.

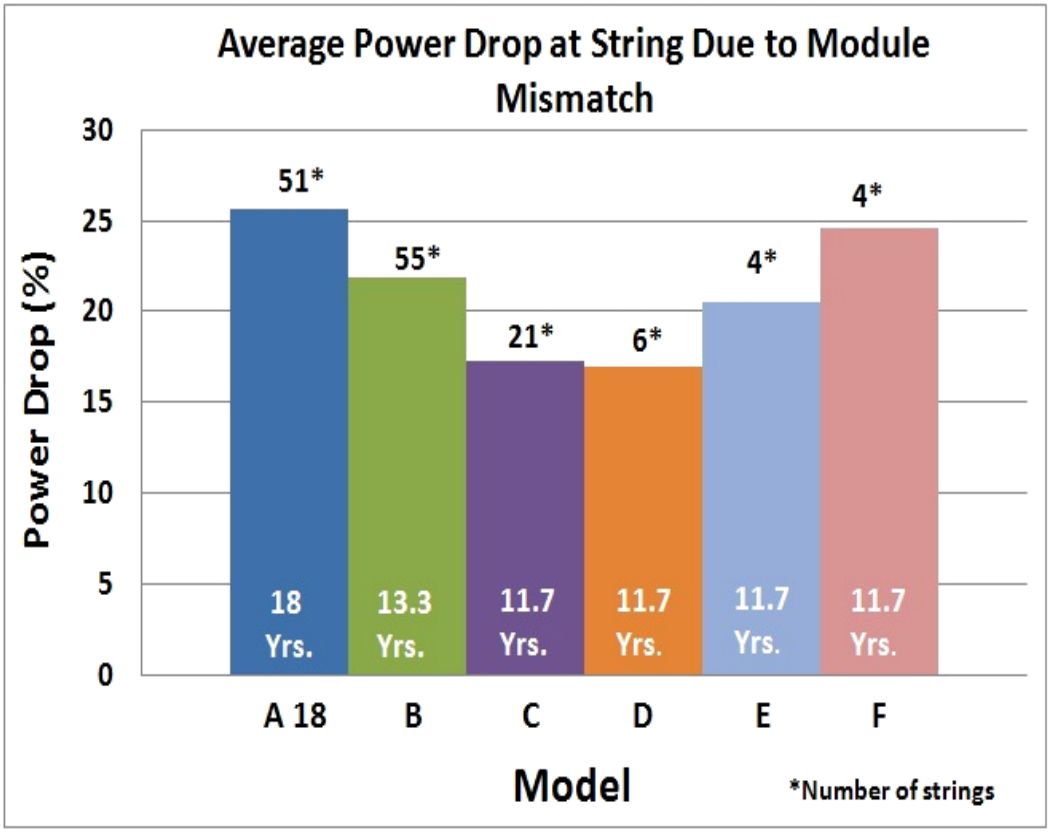

Figure 4.21 Average Power drop at string level due to module mismatch (plant)

Figure 4.21 represents the average of power drop due to mismatch at the string level. The overall average for the plant is 20.8%. This finding implies that the plant can give 20% more power output if the effects of module mismatch at string level are minimized. Twenty percent is a considerable amount, given that this is the total DC power output of the power plant. Losses due to wiring and power conversion add up to this amount, and the total plant output is affected dramatically.

4.4 Module Mismatch as seen in Individual Strings

Following is the detailed analysis of one string of each model from the module mismatch perspective. The plots included in this investigation depict two vital graphs: (1) mismatch between powers of modules in one particular string

(Primary Y-axes) and (2) comparison of total power drop due to performance degradation and, further, due to mismatch (Secondary Y-axes).

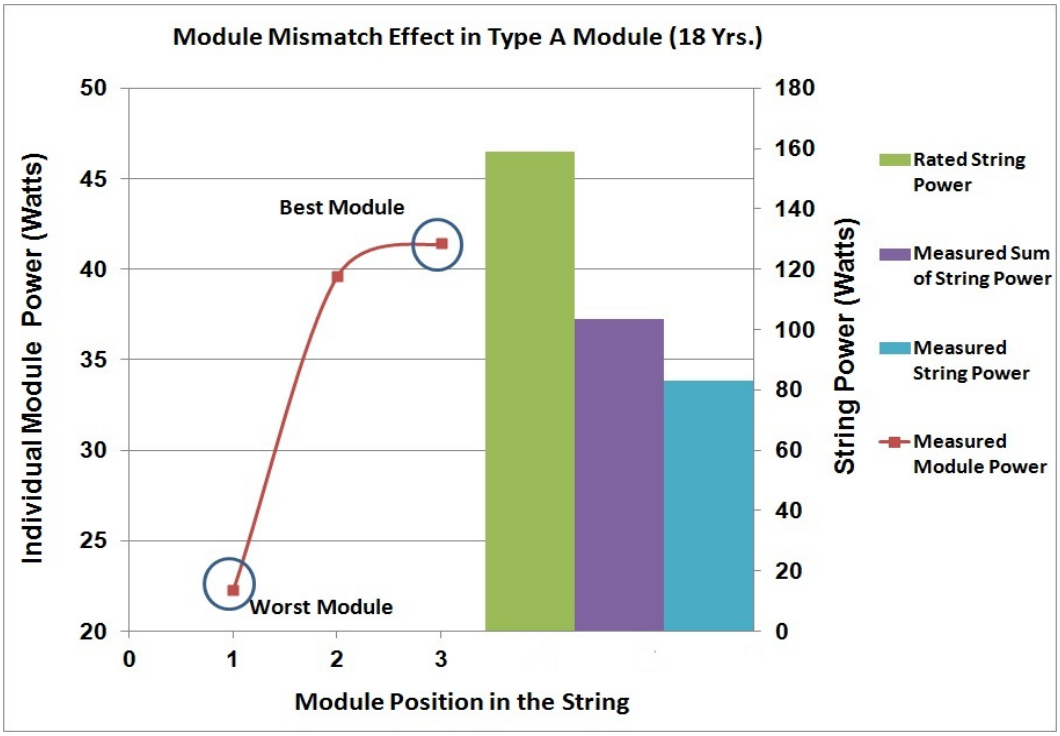

Figure 4.22 Module mismatch as seen in one of the strings of Model A

Figure 4.22 shows one of the strings of model A. A difference of approximately 20 watts can be seen between the best and the worst modules of this string. These modules were rated at 53 watts (STC). A 20% drop clearly can be attributed to ageing. A difference of 50% in the power of the best and the worst module would dictate the string power output.

As apparent from the secondary Y-axis, the string was rated to perform at 159 watts initially. The drop in the measured sum can be attributed to the performance degradation with time. A third bar depicting power drop due to mismatch effect shows that the string is actually giving an output at 50% of its rated STC power. The power drop due to degradation in this case (35%) is

higher than the power drop due to mismatch (20%), indicating that the degradation plays a higher role in the decreased performance of the string.

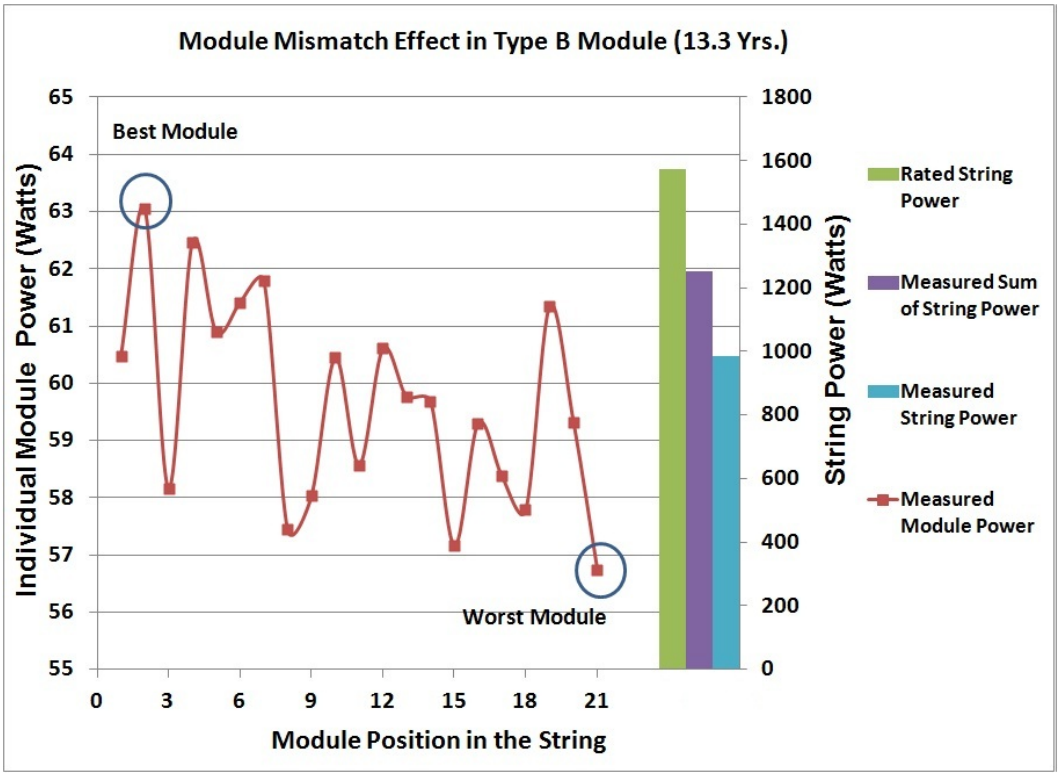

Figure 4.23 Module mismatch as seen in one of the strings of Model B

Figure 4.23 refers to model B. This model has the highest number of modules at the APS STAR power plant and is the key determining model in the average power drop at the plant level. The power output from individual modules, although not high at the string level, is sporadic throughout the string. The difference between the best and the worst module is 6 watts (approximately 10%). The age of type B is 13 years, which is less than the age of module A. As seen earlier, the performance degradation is also less in this case. All of these factors combine and produce a string power output of 995 watts, which is 36% less than the rated string power. Nonetheless, the amount of power drop has

decreased due to the younger age of these modules. The power drop due to degradation (20.5%) is similar to the power drop due to mismatch (21.5%) Considering the case of type C modules (same age group as type B) in Figure 4.24, a greater difference is seen between the best and worst module. This difference points directly to the random performance degradation levels of this module type. There may not be more peaks due to a similar performance degradation of some modules, but the presence of even one worse module curtails the power output of the whole string.

This outcome implies that the difference between the measured sum and the measured string power would be higher than the difference of rated power to measured power. The results clearly support this statement. There is a drop of 8% power from the rated to the sum string power and an 18% drop due to mismatch in the string.

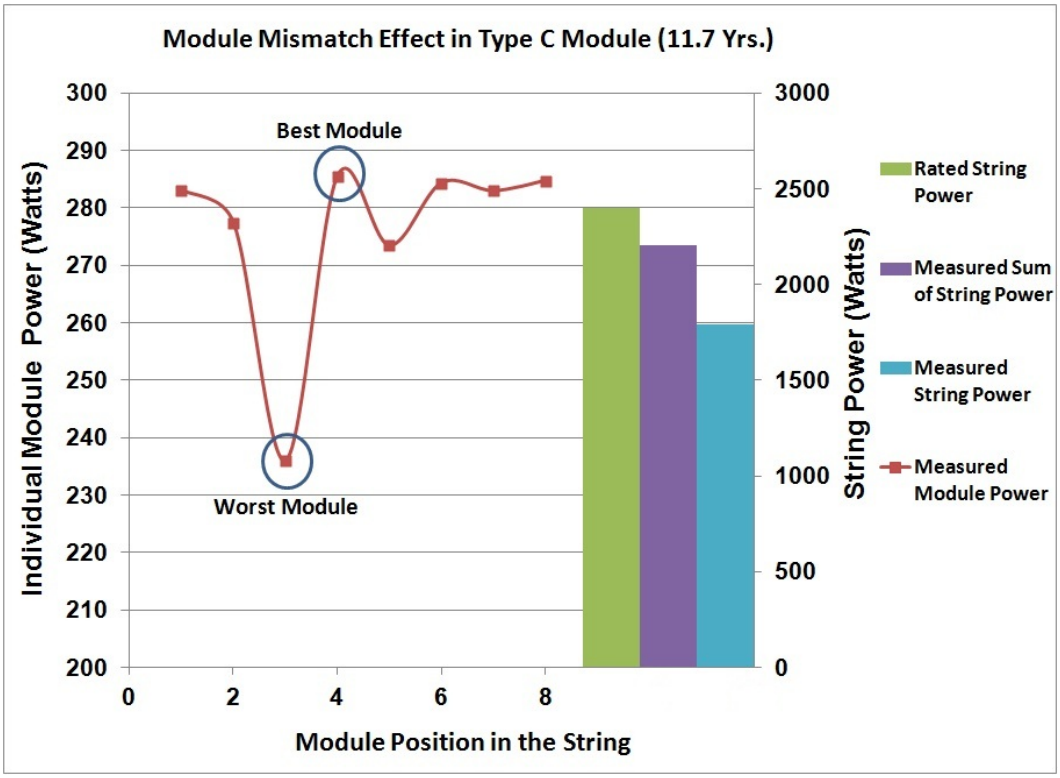

Figure 4.24 Module mismatch as seen in one of the strings of Model C

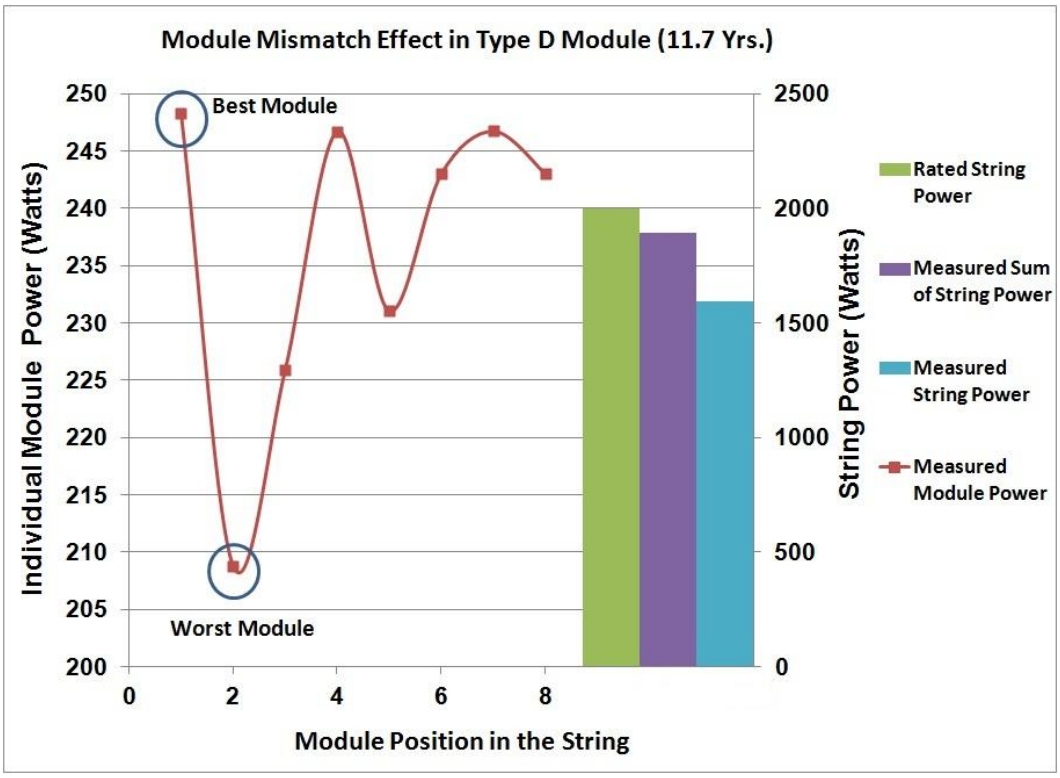

Figure 4.25 Module mismatch as seen in one of the strings of Module D

Figure 4.25 plots the individual string of type D module. Model C and D are the same age and from the same manufacturer, which explains the similarity in these plots. The power drop due to module mismatch (15%) is higher than the power lost due to degradation (5%). This advocates a more pronounced mismatch effect in these two types of modules

The plot of module E in Figure 4.26 brings about a contrasting result from modules B, C, and D, which are of similar age. A total of 12 modules are in this string arrangement. The performance degradation plot shows a descending trend towards the end of the string. The drop of STC power is not much from the rated value, but a higher mismatch factor certainly would affect the string power. The power drop due to degradation in this case was low (7 %), whereas the power drop due to mismatch was higher at 20%.

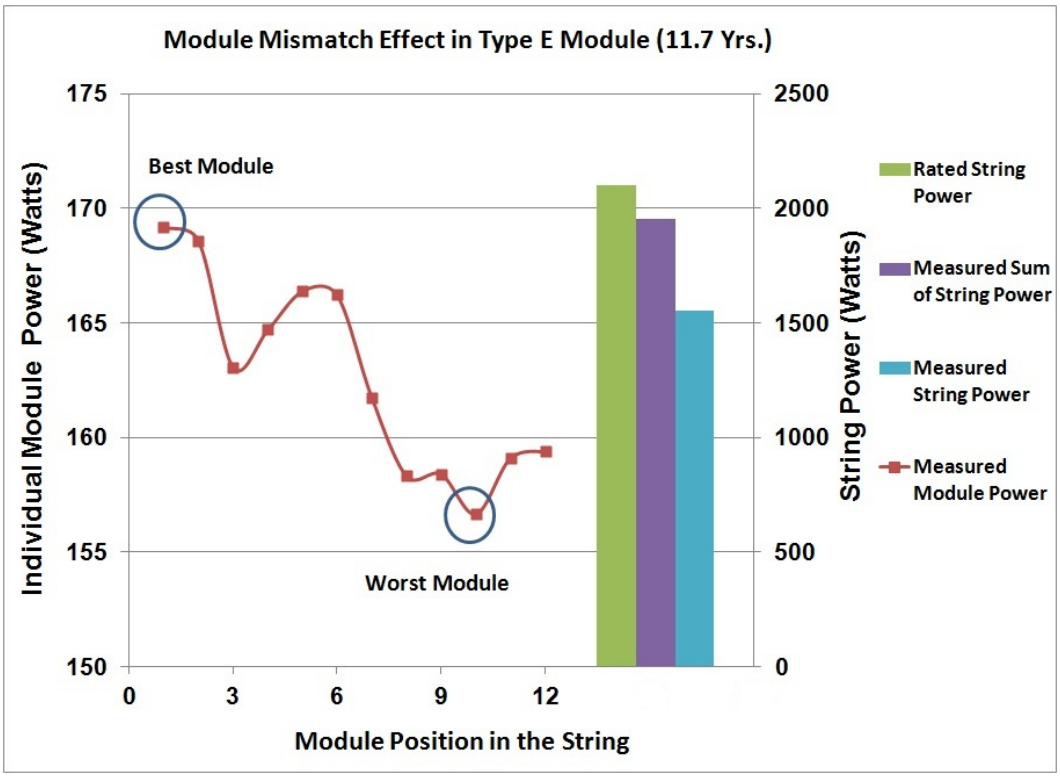

Figure 3.26 Module mismatch as seen in one of the strings of Module E

The last module type to be discussed here is the F type modules. They were seen to have the highest performance degradation among all the modules aged 11.7 years. With high average power degradation and an added effect of module mismatch, as seen in Figure 4.27, one can predict the plot on the secondary axes. Power lost in these modules due to overall degradation is 18%, and a further 28% drop occurs due to mismatch issues in the string. These percentages make the overall string perform poorly.

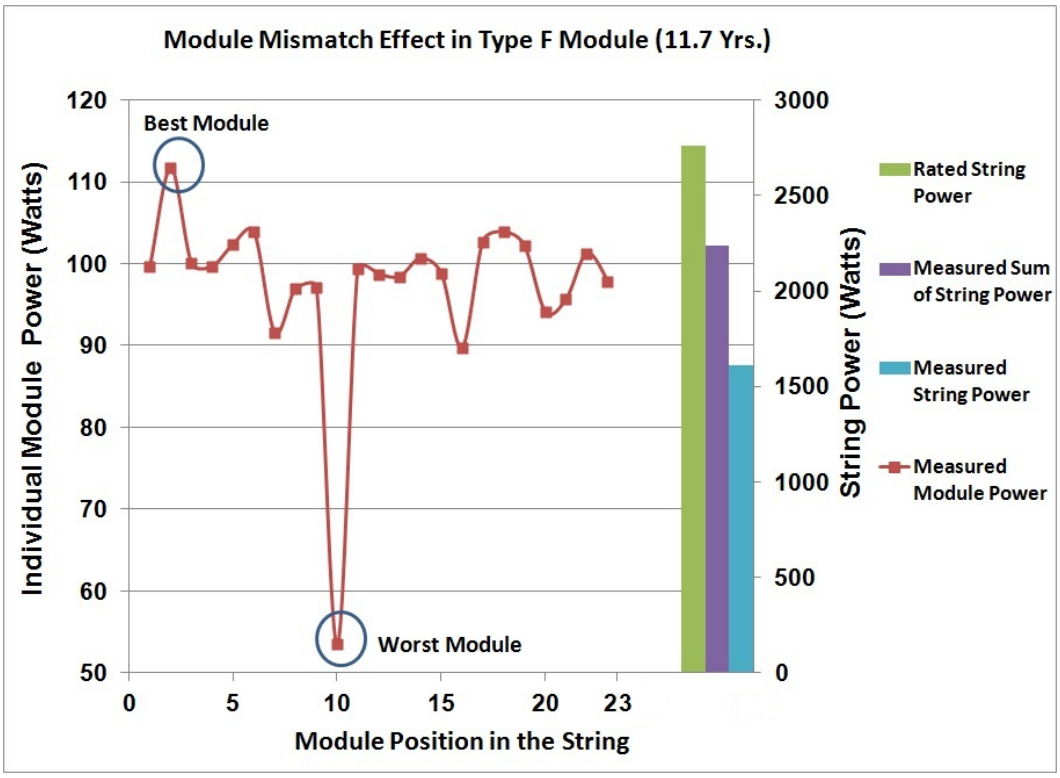

Figure 4.27 Module mismatch as seen in one of the strings of Module F

As clearly seen from all the module types plotted, a drop occurs due to degradation and then another due to mismatch issues at the string level. This leads to further underperformance of the string and, consequently, the power plant overall.

CHAPTER 5

CONCLUSIONS

5.1 Performance degradation

The data of about 1,900 field aged (12-18 years) modules shows that the average degradation rates vary from 0.6% per year to 2.5% per year. The age of a fielded module plays a vital role in the increase in degradation rate. It was also observed that modules with different designs and constructions degrade at different rates.

5.2 Potential Induced degradation

The analysis of around 1,700 modules and 133 strings spread throughout the power plant concludes that positively biased series strings do not appear to exhibit potential induced degradation. The open circuit voltages of the three kinds of strings analyzed in this study were +65 V, +455V, and +500 V. The age of the modules varied from 12 to 18 years. The degradation trends observed at string level were random, and no average degradation trend was seen at the system (same module position) level in any type of models discussed. Low relative humidity conditions of Tempe, Arizona can be a possible reason for this observation.

5.3 Power Loss due to Module Mismatch at String Level

The individual and string I-V data of 1,900 field aged modules was combined and the power output was plotted according to circuit diagrams. The decrease in output power due to module mismatch at the string level ranged between 15% and 26%. The average power drop for the power plant was about 22%. Modules aged 18 years were seen to exhibit a greater drop of power due to performance

degradation and module mismatch. The highest number of modules was found in the 13-year age group. They exhibited a similar loss in power due to degradation and mismatch. Modules aged 12 years showed that, although age had an effect on performance degradation, the effect of module mismatch became even more severe with the existence of one underperforming module in the string. Modules in this age bracket also exhibited more pronounced mismatch issues due to their random power degradation.

REFERENCES

[1] C.R. Osterwald, A. Anderberg, S. Rummel, and L. Ottoson, “Degradation Analysis of Weathered Crystalline- Silicon PV Modules," 29th IEEE PVSC, 2002

[2] M.A. Quintana, D.L. King, T.J. McMahon, and C.R. Osterwald, “Commonly observed degradation in field-aged photovoltaic modules,” 29th IEEE PVSC, 2002

[3] J.H. Wohlgemuth, “Reliability Testing of PV Modules,” First WCPEC, 1994

[4] J.H. Wohlgemuth, D.W. Cunningham, P. Monus, J. Miller, A. Nguyen, "Long Term Reliability of Photovoltaic Modules," Photovoltaic Energy Conversion, Conference Record of the 2006 IEEE 4th World Conference, vol.2, pp. 2050-2053, May 2006

[5] D.L. King, M.A. Quintana, J.A. Kratochvil, D.E. Ellibee, and B.R. Hansen, “Photovoltaic Module Performance and Durability Following Long-Term Field Exposure,” Progress in Photovoltaics, Sandia National Laboratories, Albuquerque, 2000

[6] JPL Publication 510-161, “Block V Solar Cell Module Design and Test Specification for intermediate Load Applications,” 1981

[7] Photovoltaic Reliability Class, Topic: “Failure Rates and the Bathtub Curve,” AZ, 2010

[8] IEC-61215: Crystalline silicon terrestrial photovoltaic (PV) modules-Design qualification and type approval, 2005

[9] IEC-61646: Thin film silicon terrestrial photovoltaic (PV) modules-Design qualification and type approval, 2008[10] Louis L. Bucciarelli Jr. “Power loss in photovoltaic arrays due to mismatch in cell characteristics,” Solar Energy, Volume 23, Issue 4, pp. 277-288, 1979

[11] N.D. Kaushika, and A.K. Rai, “An Investigation of Mismatch Losses in Solar Photovoltaic Cell Networks,” Energy, 32, pp. 755–759, 2007

[12] M.C. Alonso-García, J.M. Ruiz, and F. Chenlo, “Experimental study of mismatch and shading effects in the I–V characteristic of a photovoltaic module,” Solar Energy Materials and Solar Cells, Volume 90, Issue 3, pp. 329-340, 2006

[13] M. Schütze, M. Junghänel, M.B. Koentopp, S. Cwikla, S. Friedrich, J.W. Müller, P. Wawer Q-Cells, and S.E. Sonnenallee, “Laboratory study of

potential induced degradation of silicon photovoltaic modules," 37th IEEE PVSC, 2011

[14] W.I. Bower and J.C. Wiles, "Analysis of grounded and ungrounded photovoltaic systems," 24th IEEE PVSC, 1994

[15] P. Hacke, K. Terwilliger, R. Smith, S. Glick, J. Pankow, M. Kempe, and S. Kurtz, "System Voltage Potential –induced degradation mechanisms in PV modules and methods for test," 37th IEEE PVSC , 2011

[16] J. Wiles,* (March 1, 2006*), http://www.nmsu.edu, Photovoltaic Power Systems and the 2005 National Electrical Code: Suggested Practices, 10/23/2011

[17] W. Richardson, "Potential Induced Degradation," SOLON Corporation, NREL Photovoltaic Reliability Workshop, February 11, 2011

[18] N.G. Dhere, S.A. Pethe, A. Kaul, "High Voltage Bias Testing of Specially Designed c-Si PV Modules," Proc. SPIE, 2011

[19] P. Hacke, K. Terwilliger, S. Glick, M. Kempe, S. Kurtz, I. Bennett, and M. Kloos, "Requirements for a Standard Test to Rate the Durability of PV Modules at System Voltage," NREL Photovoltaic Module Reliability Workshop, 2011

[20] A. Suleske, J. Singh, J. Kuitche, and G. Tamizh-Mani, "Performance degradation of grid-tied photovoltaic modules in a hot-dry climatic condition," Proc. SPIE, 2011